KU LEUVEN

Signatures of nuclear structure changes in neutron-rich Cr isotopes

Robbe Van Duyse, KU Leuven

dr. L. Lalanne, Université de Strasbourg CNRS, CERN, KU Leuven

Prof. dr. Á. Koszorús, KU Leuven

Prof. dr. G. Neyens, KU Leuven

For the CRIS collaboration

LISA Conference 2024

Introduction to the nuclear shell model

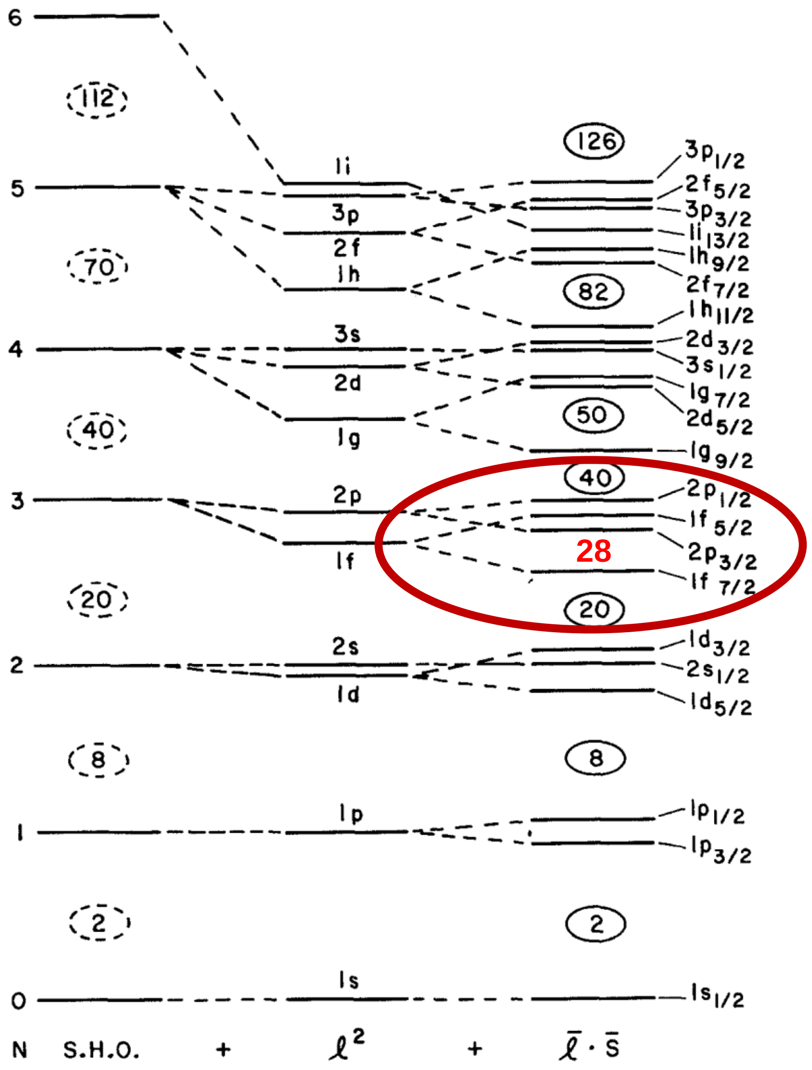

fp-shell

$^{51-61}\mathrm{Cr}$

Z = 24 N = 27 - 37

All valence neutrons
lie in fp-shell

Cr between the Ni and Ca isotopic chains

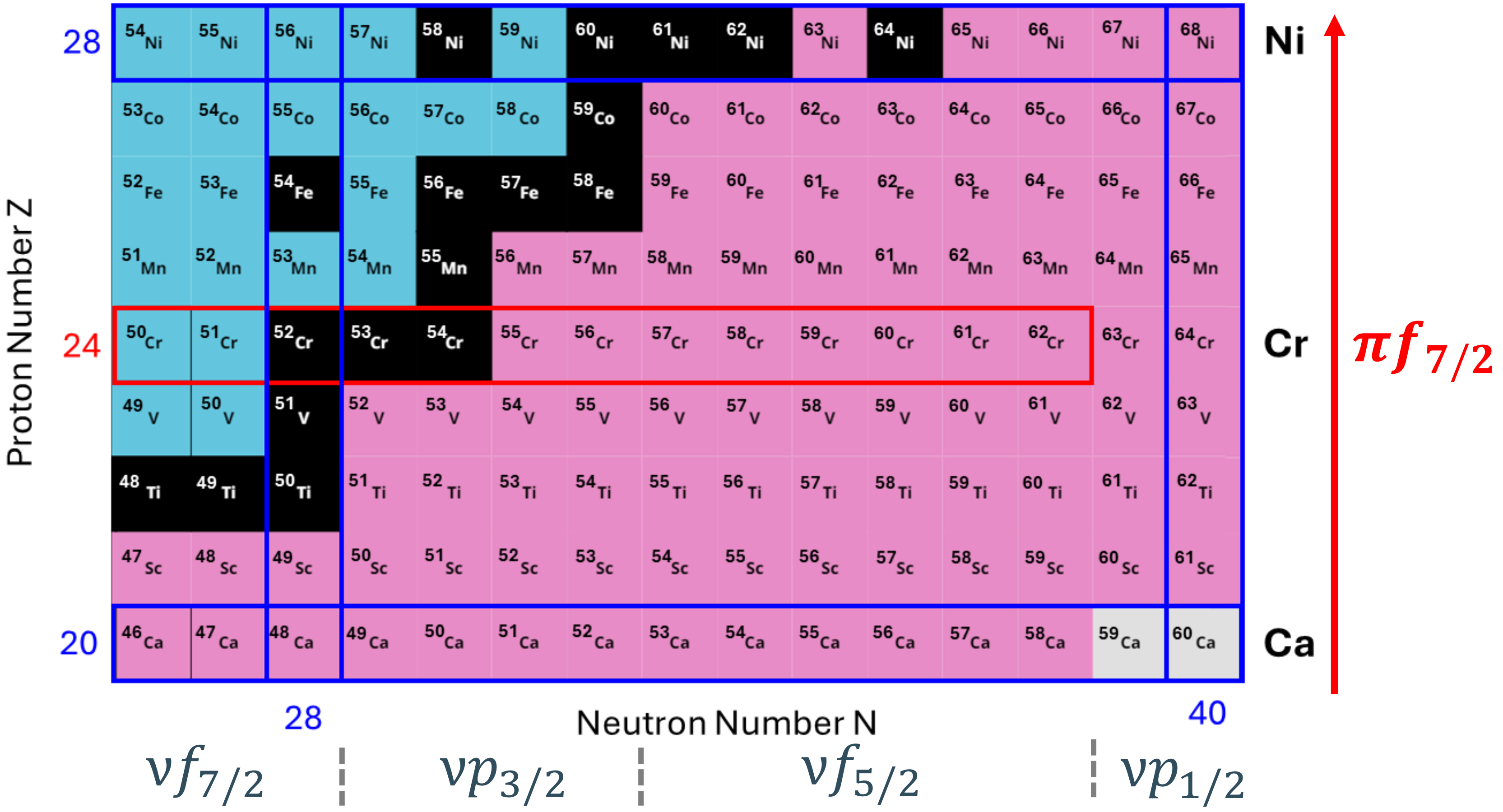

Studied $^{50-62}\mathrm{Cr}$

Cr (*Z*=24) inbetween
Ca (*Z*=20) and Ni (*Z*=28)

Middle of 2 magic proton shell closures

Shell structure evolution from Ca to Ni

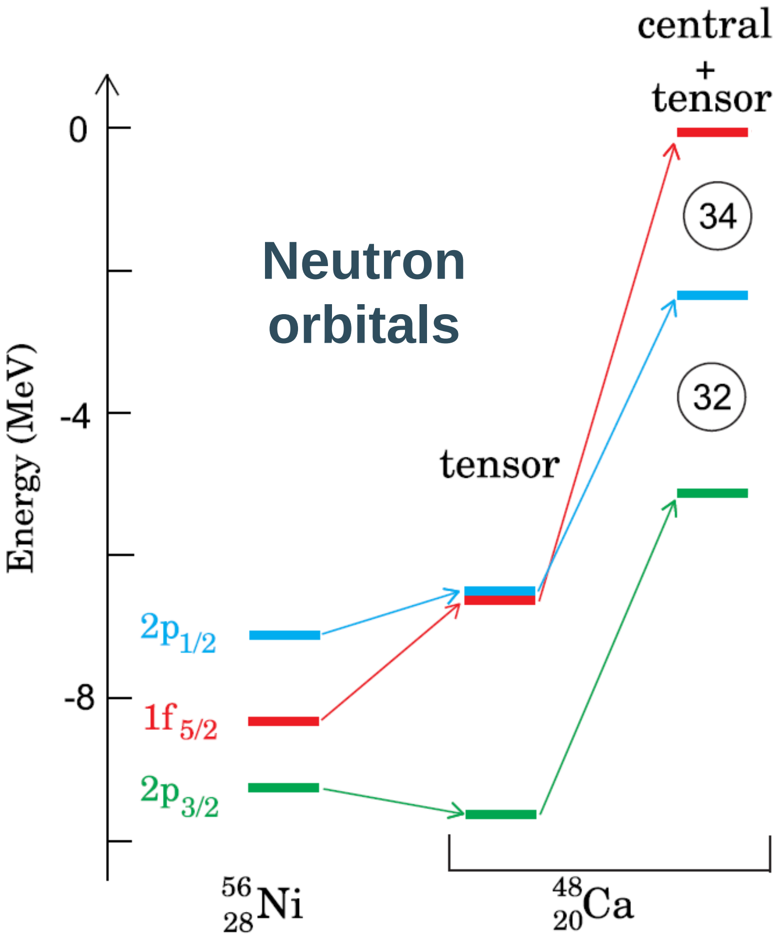

$\pi f_{7/2}$

From **theoretical calculations**

Clear crossing of the $\nu f_{5/2}$ and $\nu p_{1/2}$ orbitals

New subshell gap formation at *N*=32, 34 in Ca

T. Otsuka et al. 2020

Figure taken from T. Otsuka, A. Gade, O. Sorlin, T. Suzuki, and Y. Utsuno, “Evolution of shell structure in exotic nuclei,” Reviews of Modern Physics, vol. 92, no. 1, Mar. 2020, issn: 15390756. doi: 10.1103/RevModPhys.92.015002.

Shell structure evolution from Ca to Ni

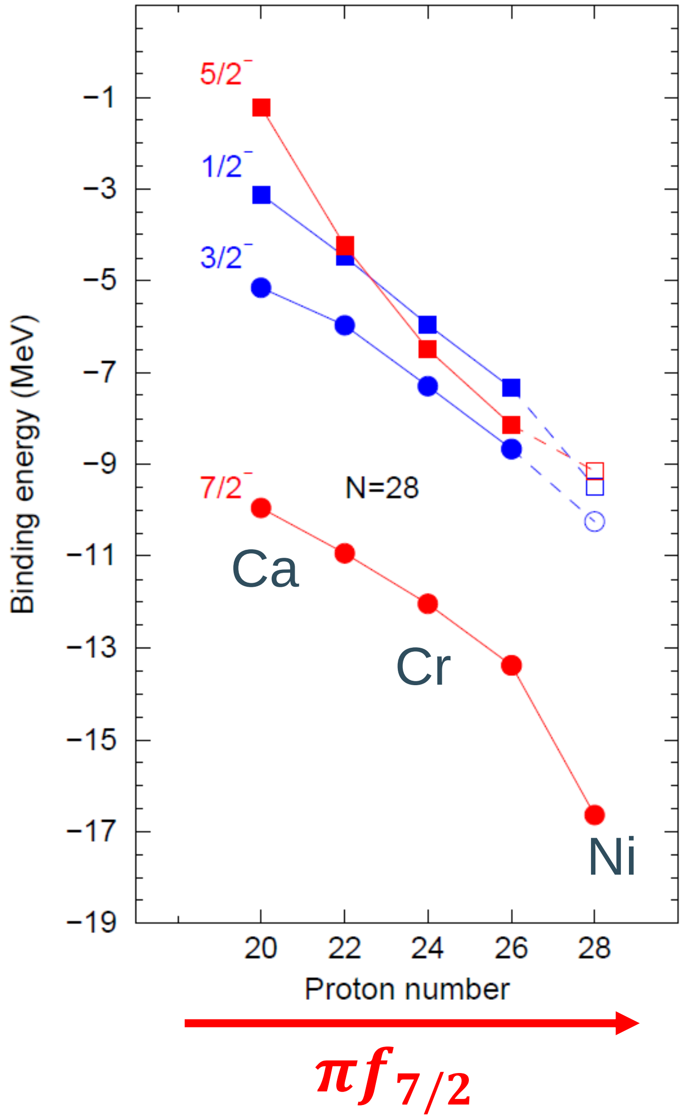

From **experimental results**

Clear crossing of the $\nu f_{5/2}$ and $\nu p_{1/2}$ orbitals

New subshell gap formation at *N*=32, 34 in Ca

O. Sorlin et al. 2008

Figure taken from O. Sorlin and M. Porquet, “Nuclear magic numbers: new features far from stability,” May 2008. doi: 10 . 1016 / j . ppnp . 2008 . 05 . 001. [Online]. Available: http : / / arxiv.org/abs/0805.2561%20http://dx.doi.org/10.1016/j.ppnp.2008.05.001

Nuclear shell structure in Cr

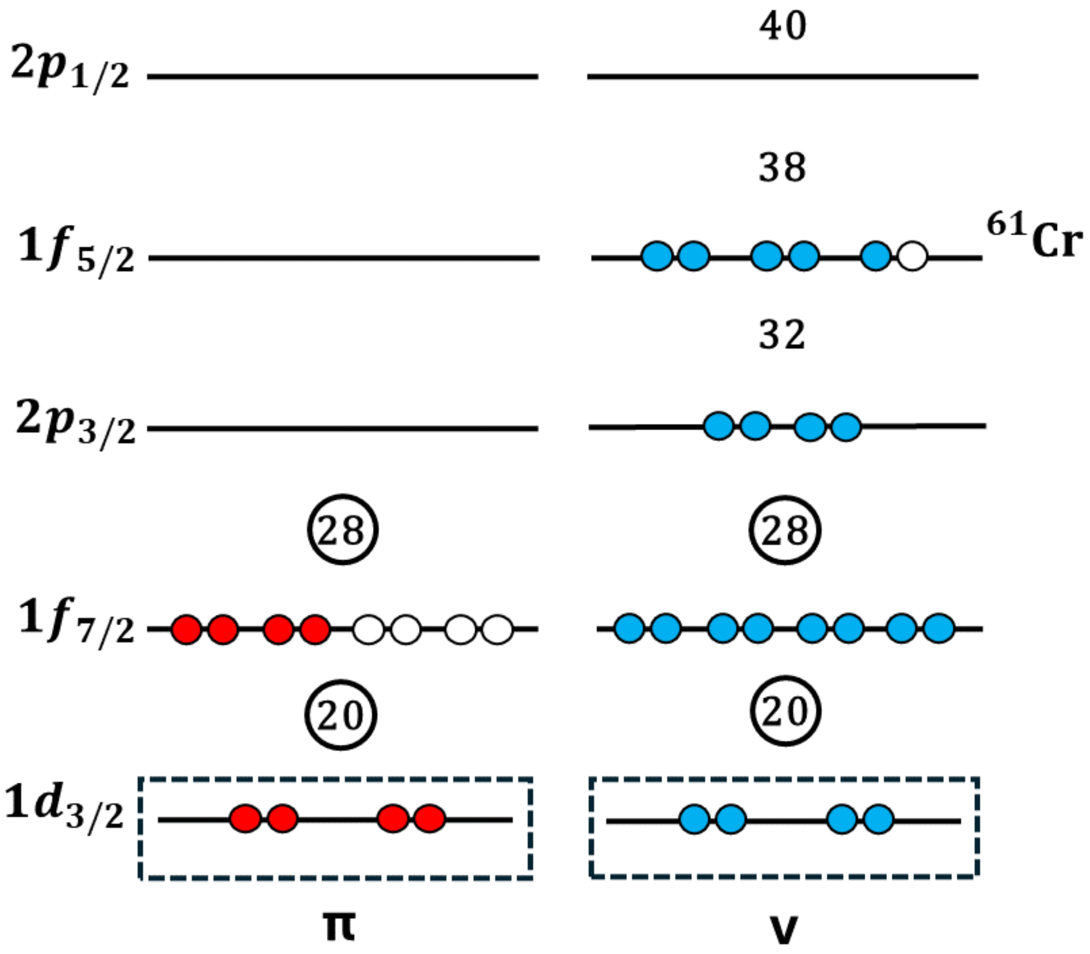

Unnuanced orbital filling and single-particle behaviour

	Literature
• 51 → 7/2	• 51 → $7/2^-$ measured
• 53 → 3/2	• 53 → $3/2^-$ measured
• 55 → 3/2	• 55 → $3/2^-$ measured
• 57 → 5/2	• 57 → $3/2^-$ tentative
• 59 → 5/2	• 59 → $1/2^-$ tentative
• 61 → 5/2	• 61 → $5/2^-$ tentative

KU LEUVEN

Observables to investigate

Nuclear ground State Spin *I*

even-even → 0^+

even-odd → depends on specific configuration of neutrons

Nuclear magnetic dipole moment *μ*

$$\mu = gI\mu_N.$$

Interaction of nucleus with magnetic fields

g-factor sensitive to specific configuration

RMS Charge Radius $<r_c^2>$

Further interpretation necessary

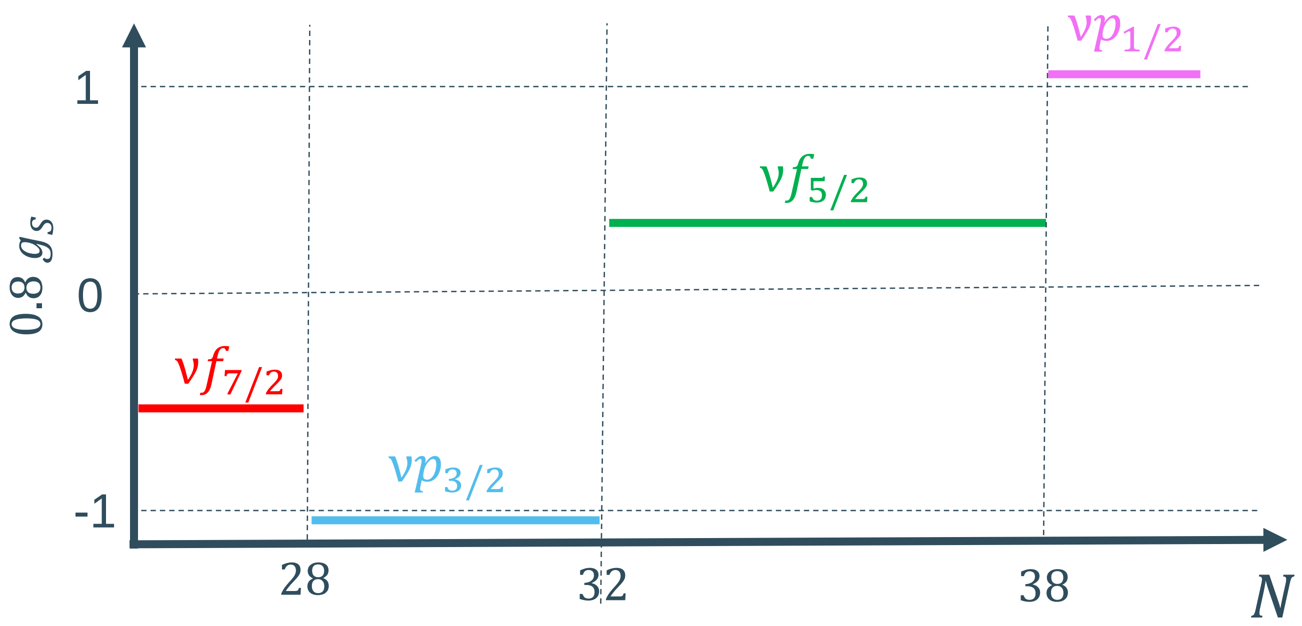

Experimental Method

Hyperfine Structure (HFS)

Interaction of the nuclear charge and current distribution with the electromagnetic fields of atomic electrons

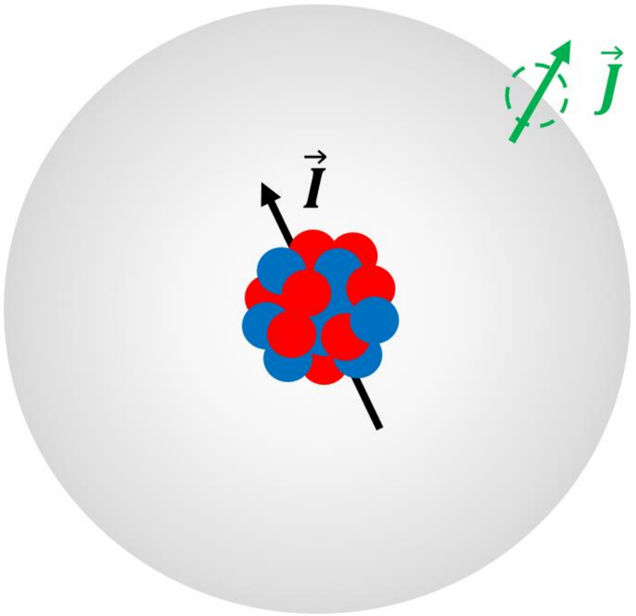

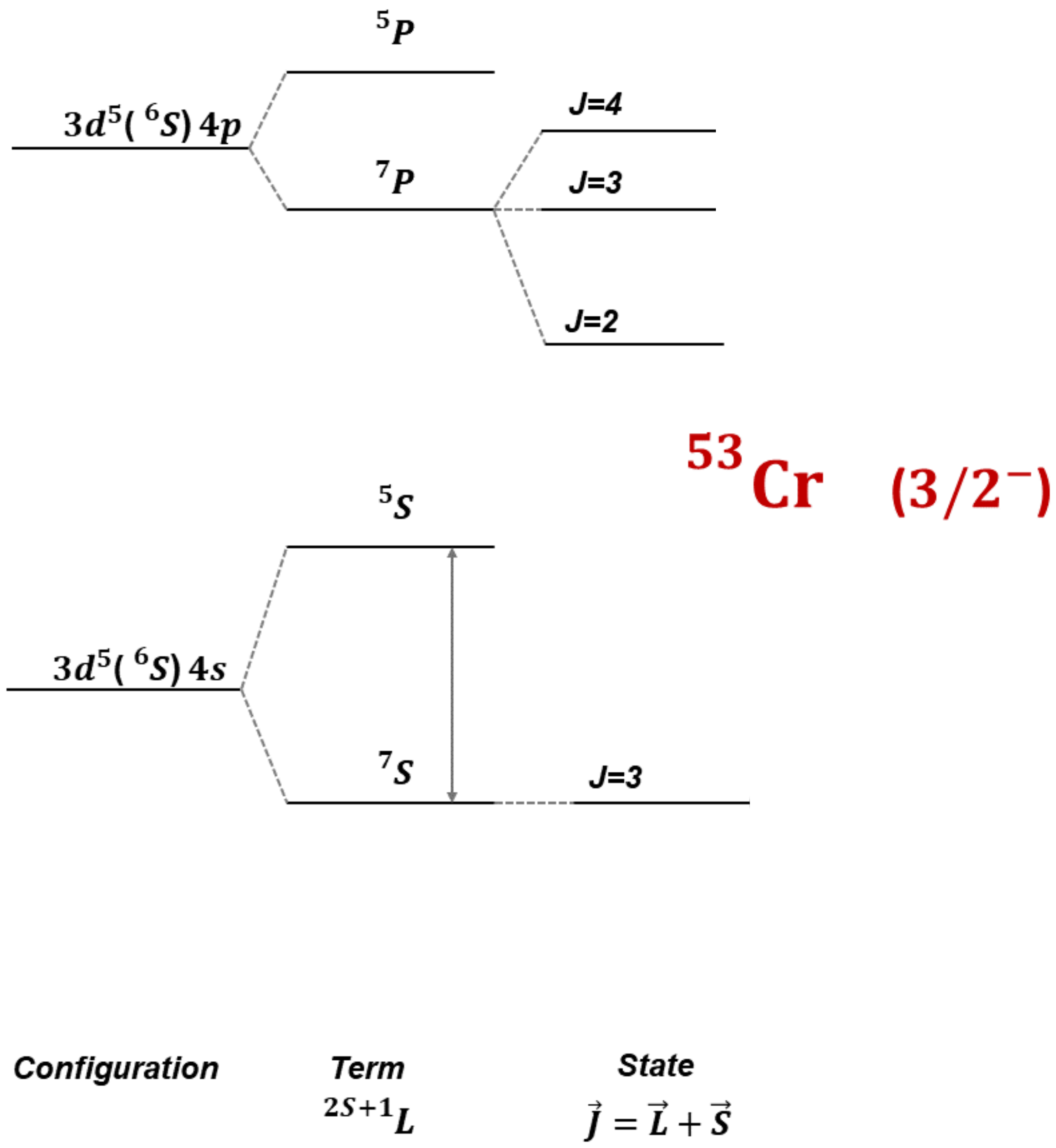

A. Kramida, Y. Ralchenko, J. Reader, and NIST ASD Team (2023), NIST Atomic Spectra Database (version 5.11), [Online]. Available: https://physics.nist.gov/asd [Wed Apr 10 2024]. National Institute of Standards and Technology, Gaithersburg, MD. DOI: https://doi.org/10.18434/T4W30F.

Hyperfine Structure (HFS)

Nuclear Spin

$$\vec{F} = \vec{I} + \vec{J}$$

Number of levels dictated by coupling

$$|I - J| \leq F \leq I + J$$

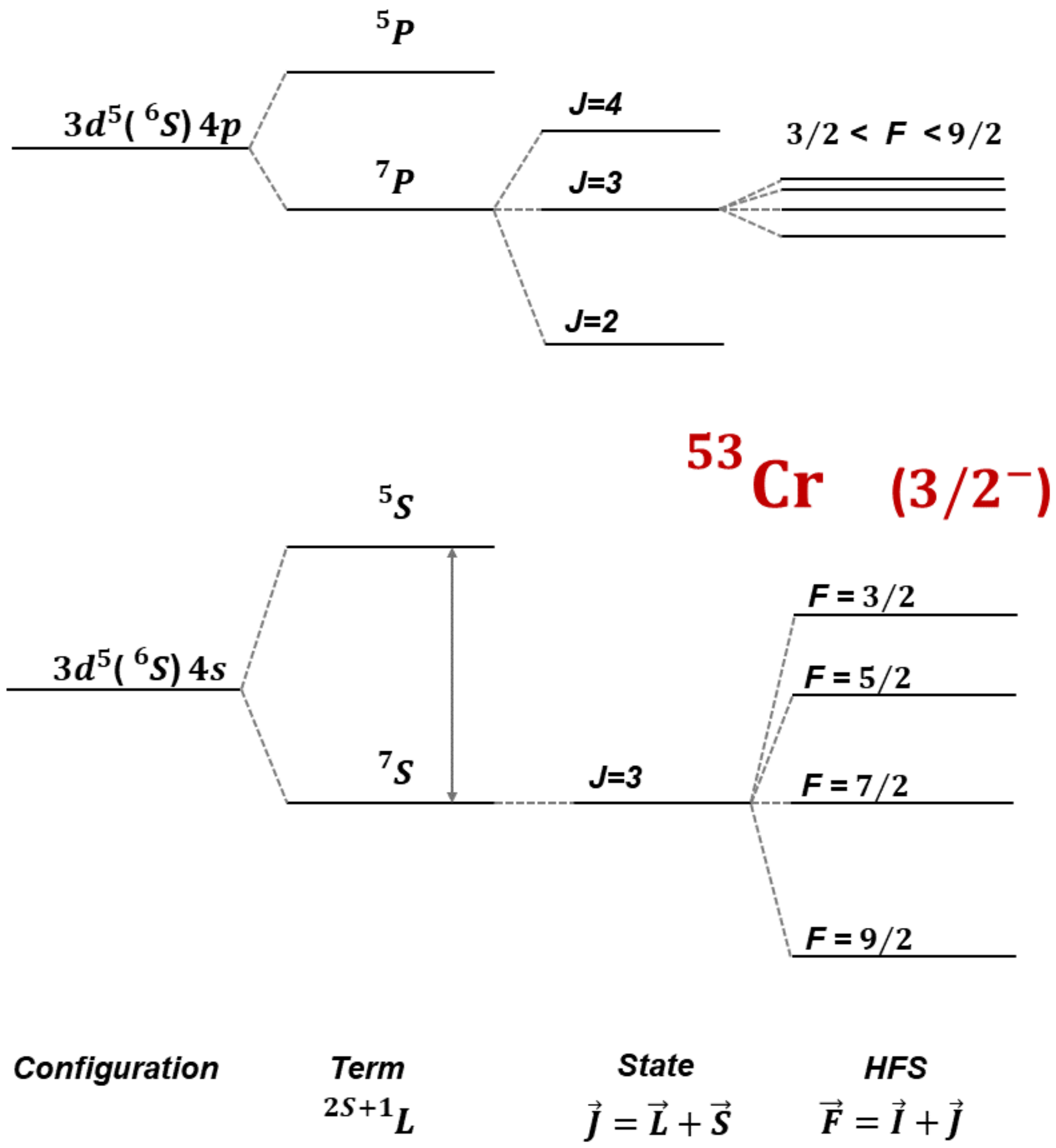

Hyperfine Structure (HFS)

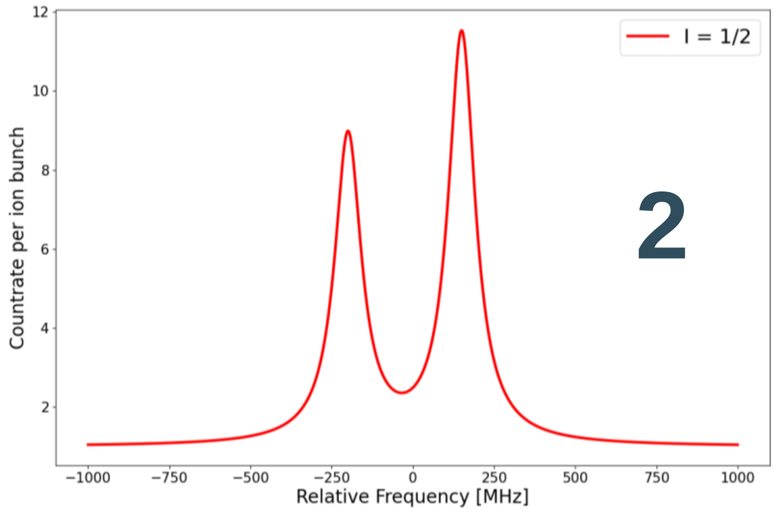

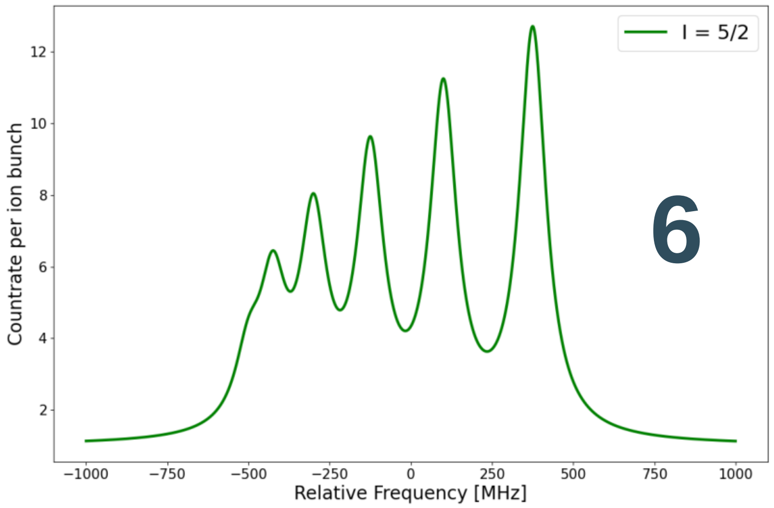

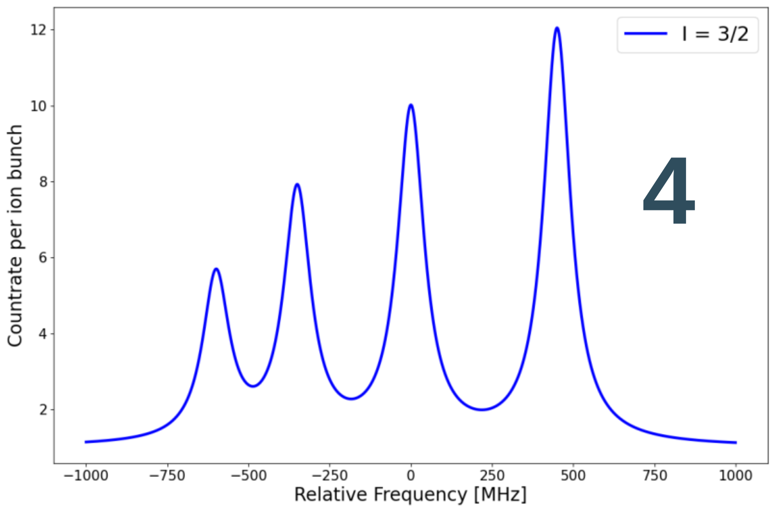

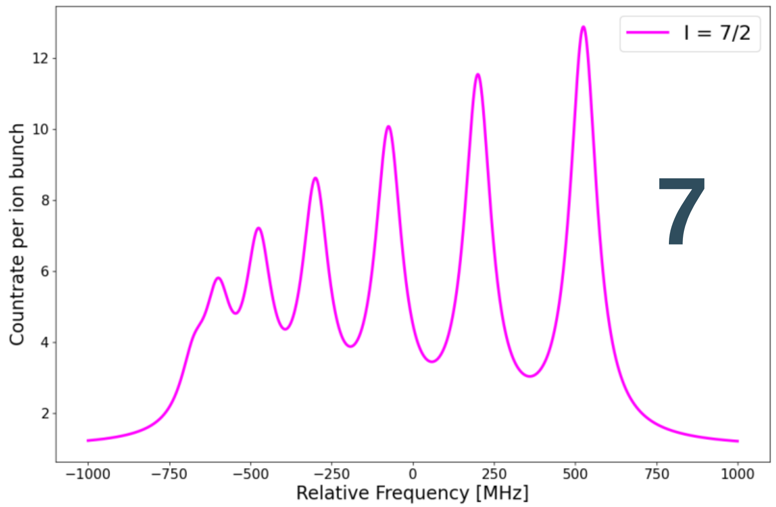

Hyperfine Structure (HFS)

$^{53}\mathrm{Cr} \quad (3/2^{-})$

Magnetic Dipole Moment

Interaction with magnetic field of electrons at center of nucleus B_0

$$U = -\vec{\mu} \cdot \vec{B}.$$

Splitting proportional to HF A parameter
→ Proportional to g-factor

$$\Delta E_{M1}(F) = -\frac{AC}{2} \quad A = \frac{\mu B_0}{\hbar^2 I J}$$

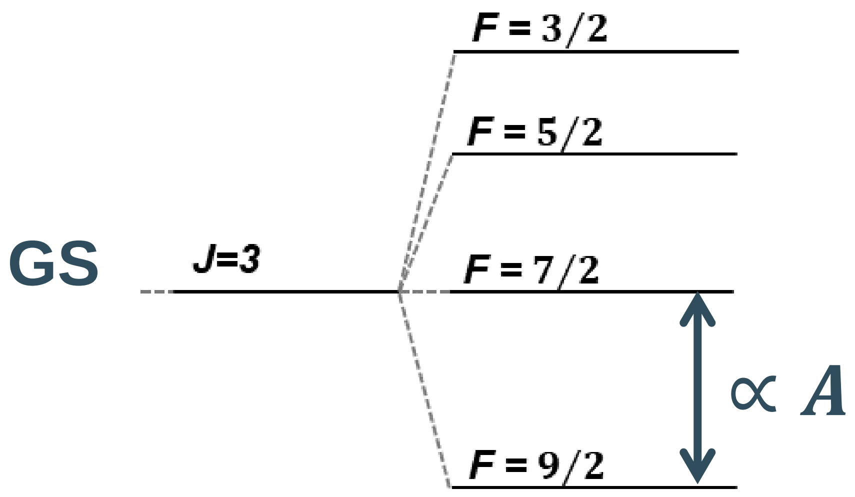

State	HFS
$\vec{J} = \vec{L} + \vec{S}$	$\vec{F} = \vec{I} + \vec{J}$

Collinear Resonance Ionization Spectroscopy (CRIS)

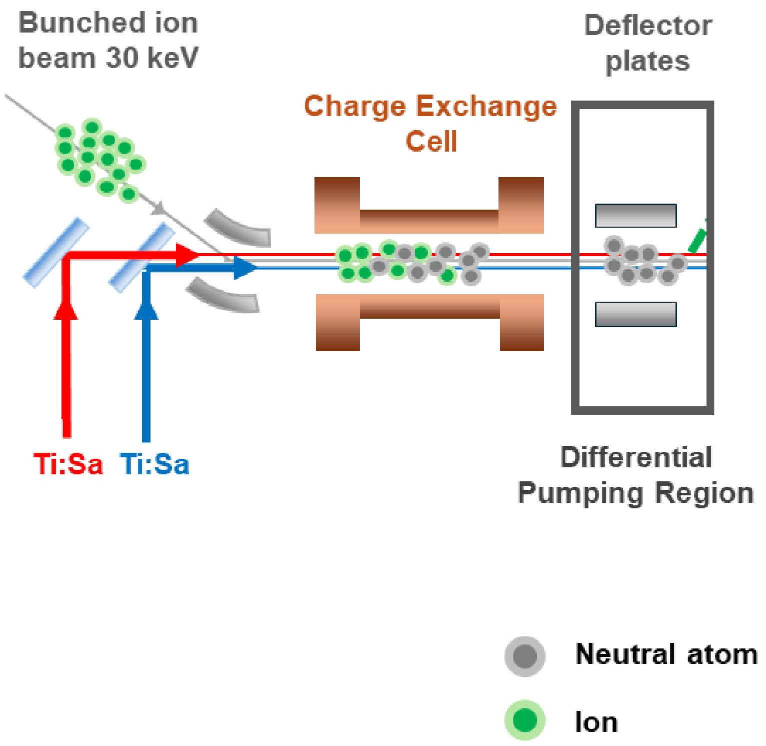

- Receive bunched and cooled Cr-ions
- HFS is atomic structure → Neutralize the beam
- Deflect remaining ions

Spectroscopic transition

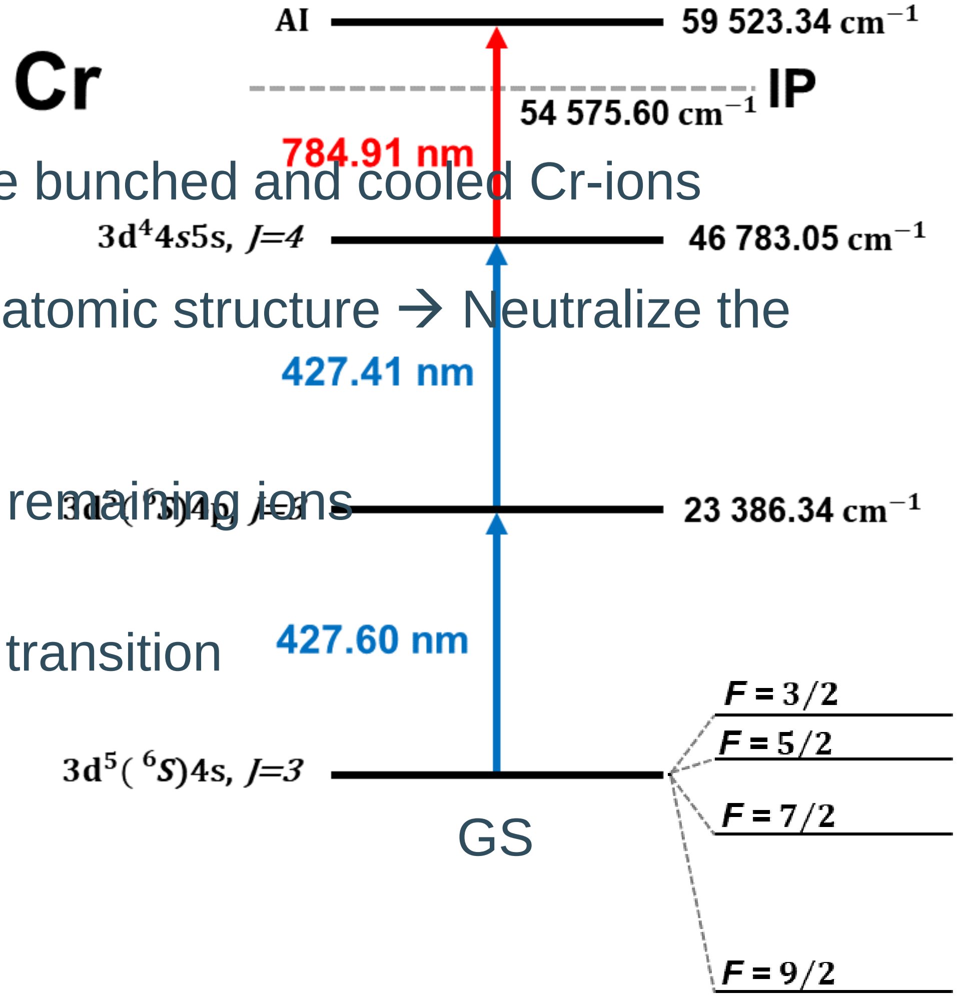

Collinear Resonance Ionization Spectroscopy (CRIS)

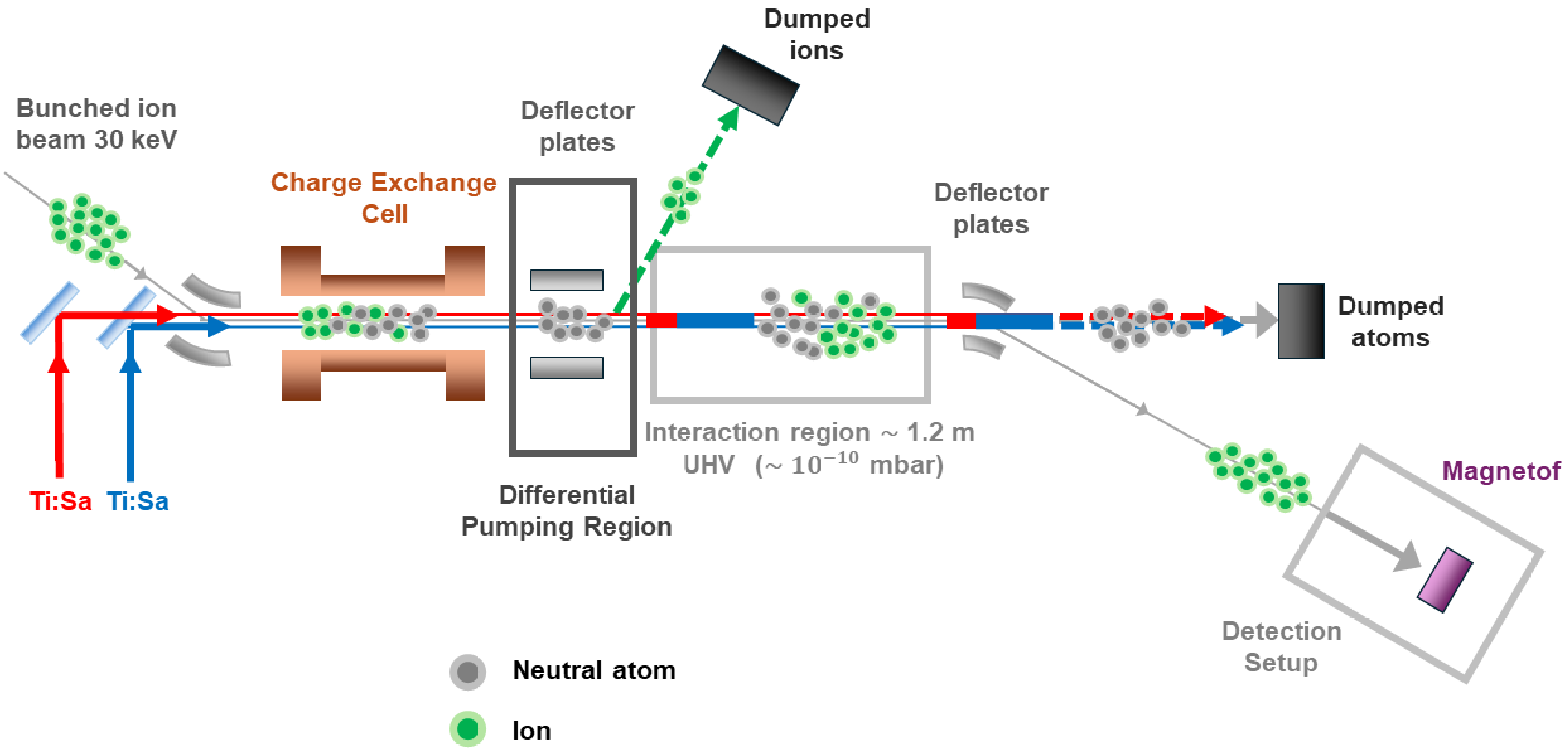

Ions detected when spectroscopic step on resonance

Resolve HFS

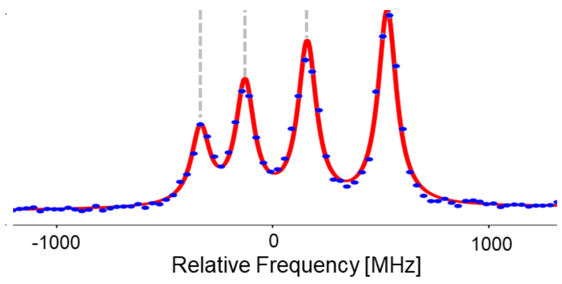

Collinear Resonance Ionization Spectroscopy (CRIS)

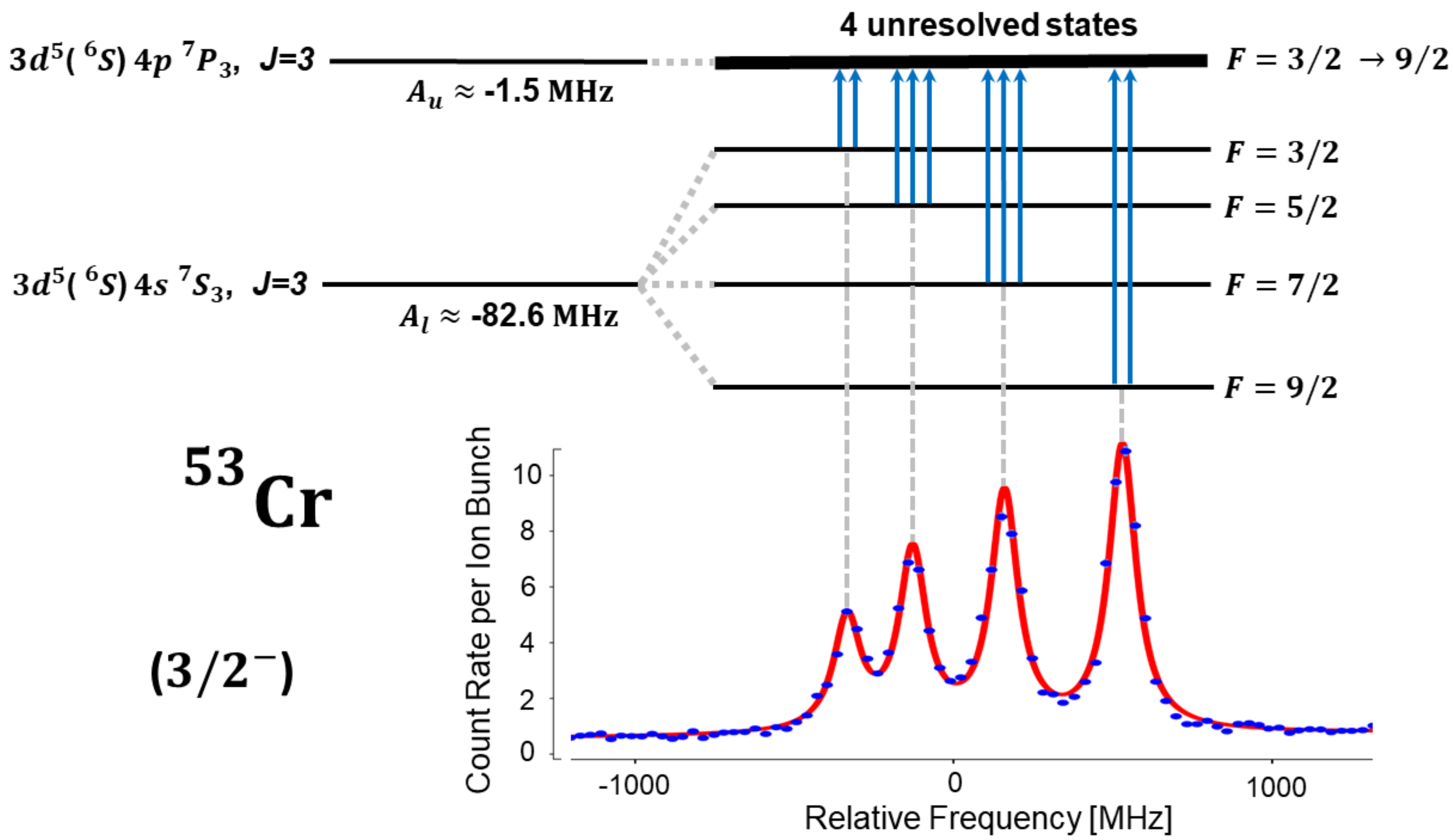

^{53}Cr

$(3/2^-)$

Resolve the HFS of the ground state

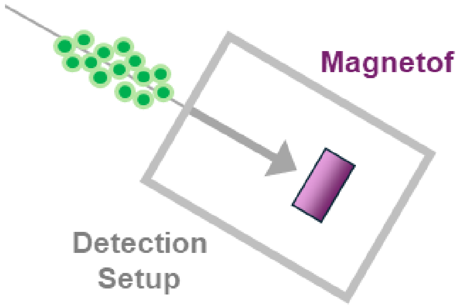

Ground state spins

$^{51,53,55}Cr$

All behave as expected, both according to orbital filling and compared to literature

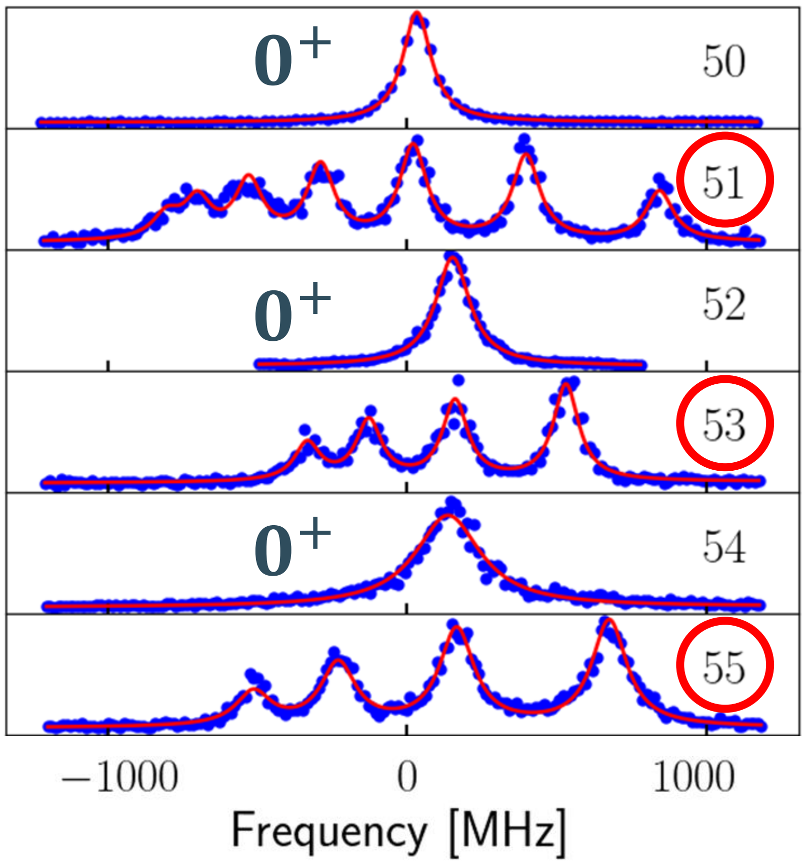

I Lit	I CRIS
$7/2^-$	$7/2^-$
$3/2^-$	$3/2^-$
$3/2^-$	$3/2^-$

^{57}Cr $\quad N = 33$

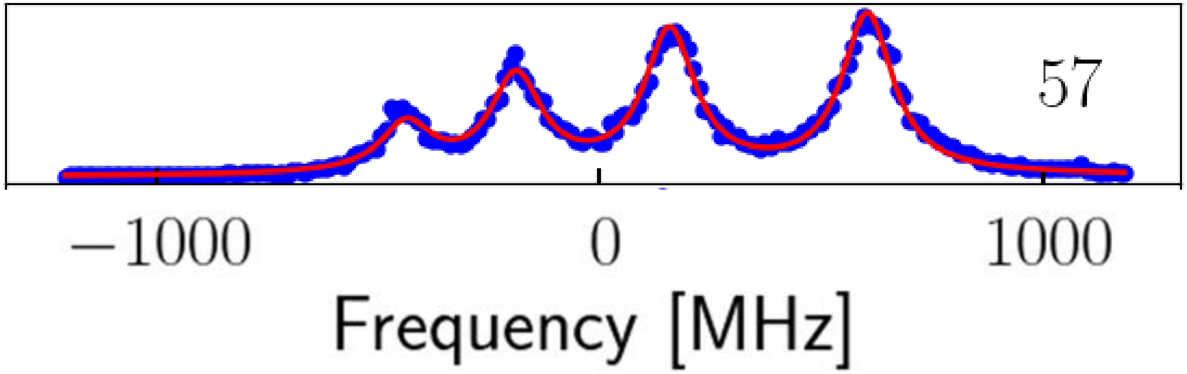

From 57 onwards expect to fill the $\nu f_{5/2}$ orbital and therefore have a spin 5/2

Not the case, CRIS confirms literature 3/2 spin

I Lit	I CRIS
$(3/2)^-$	$3/2^-$

^{59}Cr $\quad N = 35$

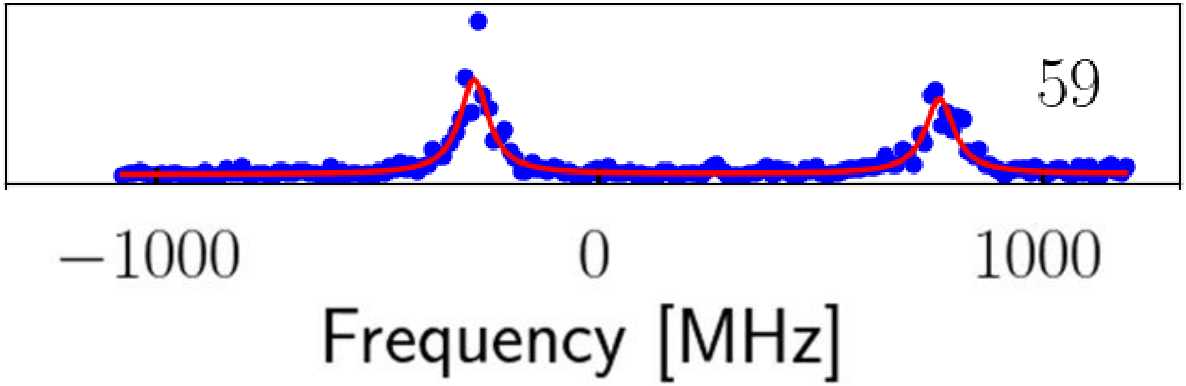

Naively expect 3 neutrons in $\nu f_{5/2}$ orbital

Correctly predicted spins by shell model calculations GXPF1A and KB3G

I Lit	I CRIS
$(1/2)^-$	$1/2^-$

$$^{59}\mathrm{Cr} \quad 1/2^- \quad (1f_{7/2})^8, (2p_{3/2})^4, (1f_{5/2})^2, (1p_{1/2})^1$$

^{61}Cr $N = 37$

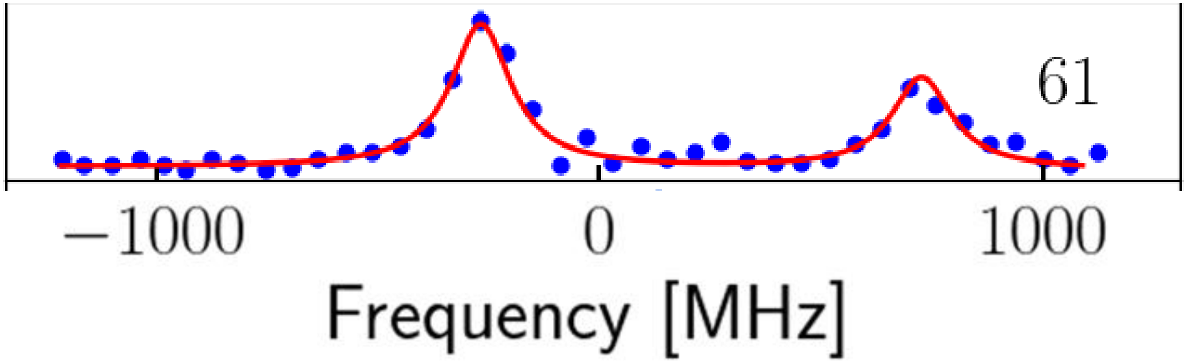

Spin 5/2 most likely configuration according to three previous publications

H.L. Crawford et al. 2009

All use β- and γ-decay spectroscopy

I Lit	I CRIS
$(5/2)^-$	$1/2^-$

^{61}Cr $\quad N = 37$

H.L. Crawford et al. 2009

Both ^{61}Mn and ^{61}Cr ground state spins only tentatively assigned

$5/2^-$ spin of ^{61}Mn confirmed at COLLAPS C. Babcock et al. 2015

$\log ft = 5.1(2)$ → (super)allowed transition

NOT supporting $\nu p_{1/2} \rightarrow \pi f_{7/2}$

→ **Pandemonium effect**

overestimating transition strengths

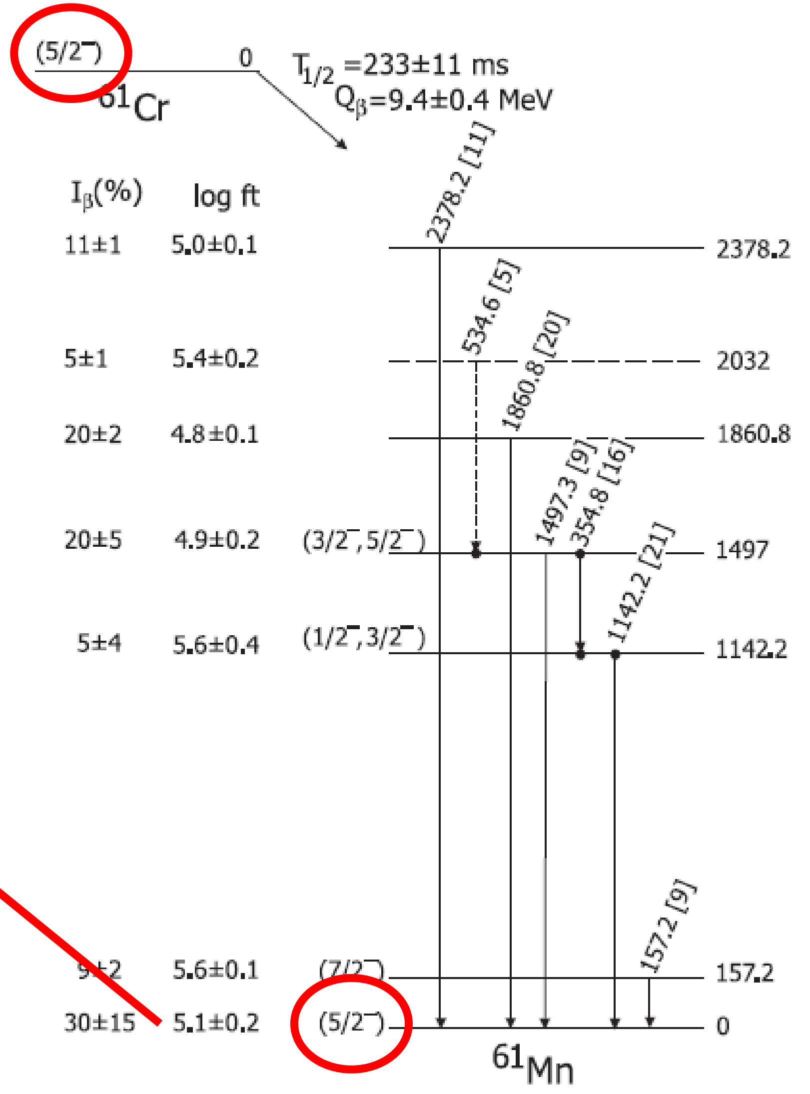

g-factors

$$g = \frac{\mu}{I}$$

g-factors

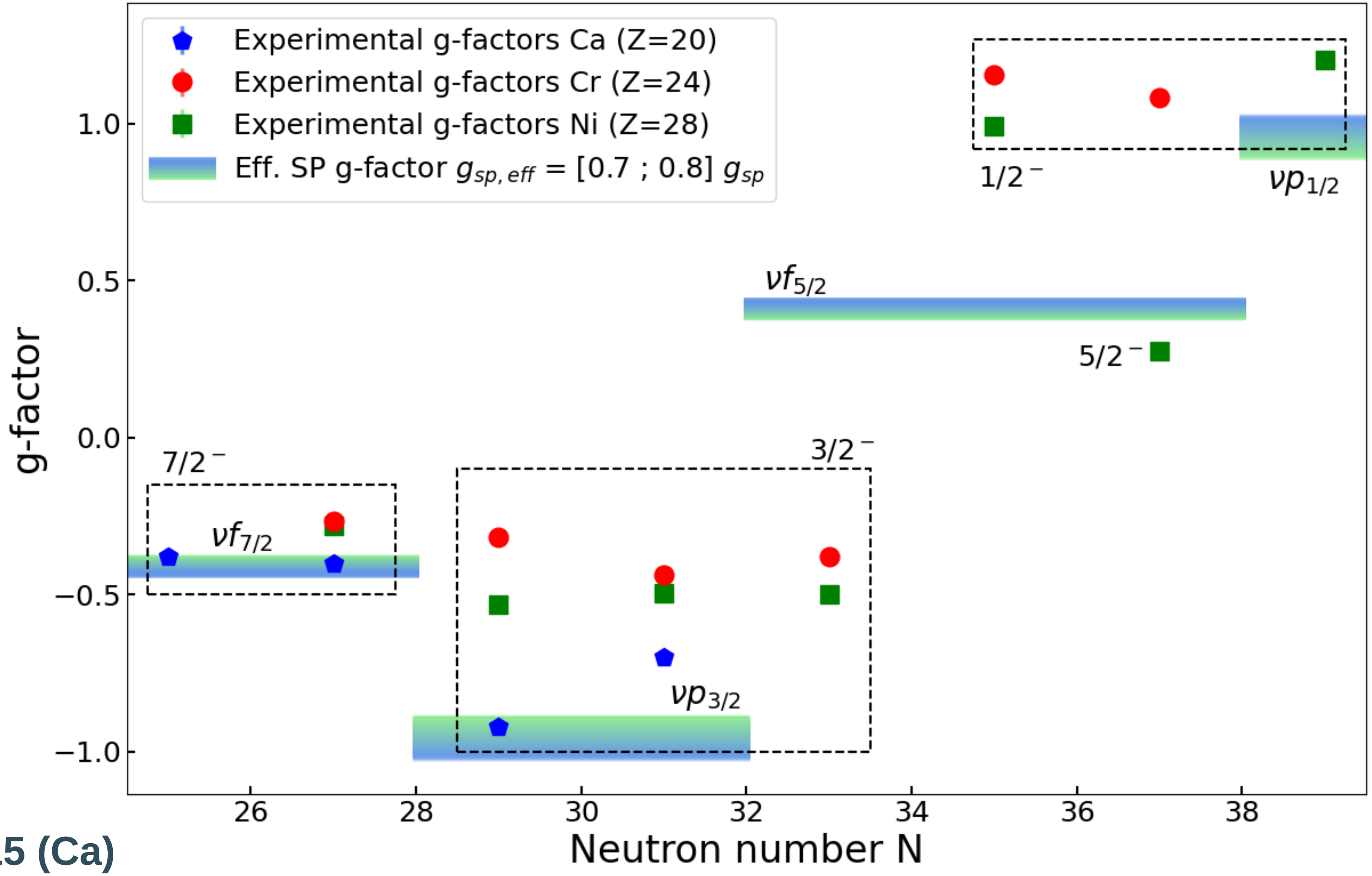

R.F. Ruiz et al. 2015 (Ca)
P. Müller et al. 2024 (Ni)

R. F. Ruiz, M. L. Bissell, K. Blaum, et al., "Ground-state electromagnetic moments of calcium isotopes," Physical Review C - Nuclear Physics, vol. 91, no. 4, Apr. 2015, issn: 1089490X. doi: 10.1103/PhysRevC.91.041304.

P. Müller, S. Kaufmann, T. Miyagi, et al., "Electromagnetic moments of the oddmass nickel isotopes 59\67Ni," Physics Letters B, vol. 854, p. 138 737, Jul. 2024, issn: 03702693. doi: 10 . 1016 / j . physletb . 2024 . 138737. [Online]. Available: https://linkinghub.elsevier.com/retrieve/pii/S0370269324002958.

^{51}Cr

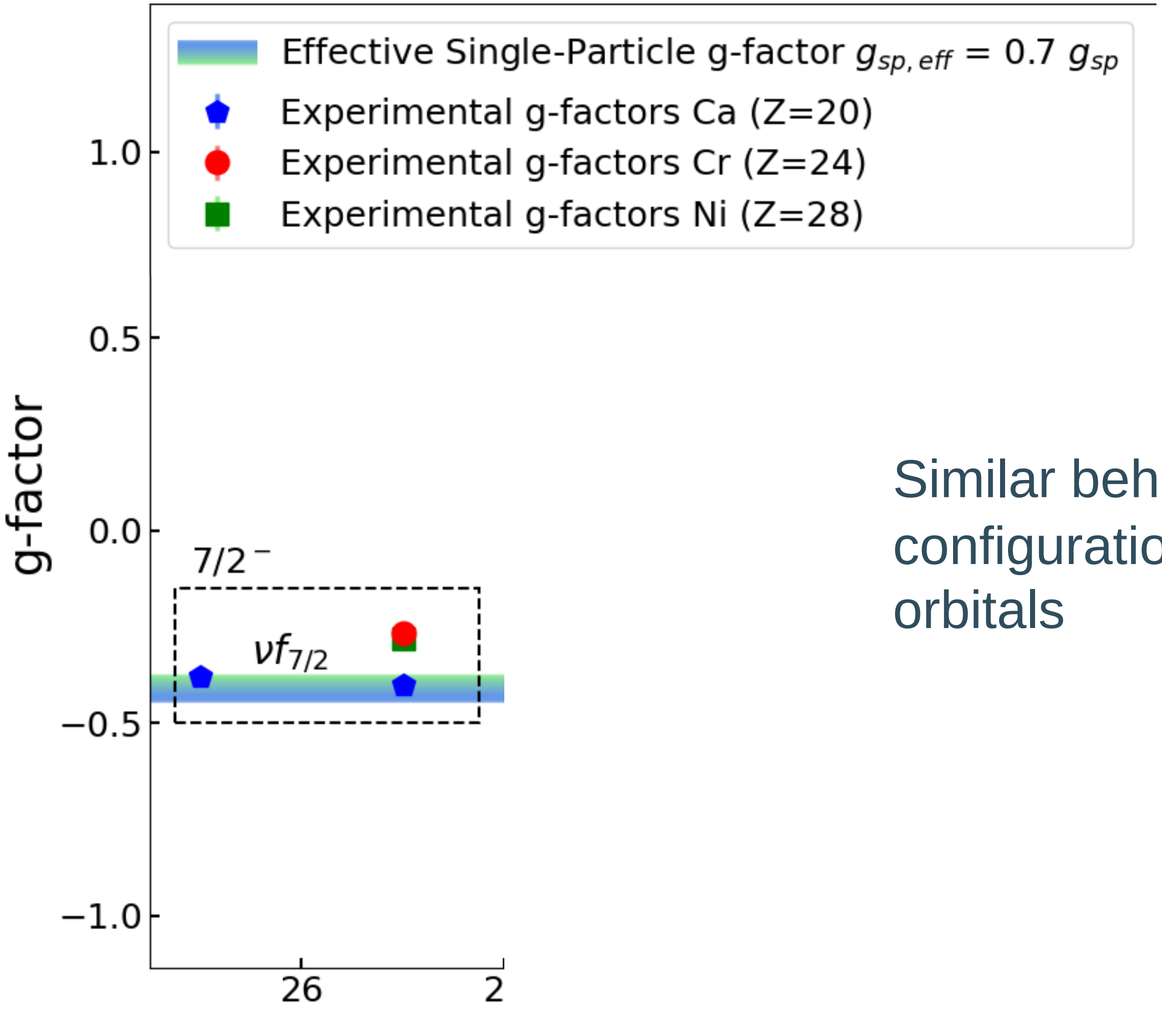

Similar behaviour to ^{55}Ni, slight configuration mixing with higher neutron orbitals

KU LEUVEN

$^{53,55,57}Cr$

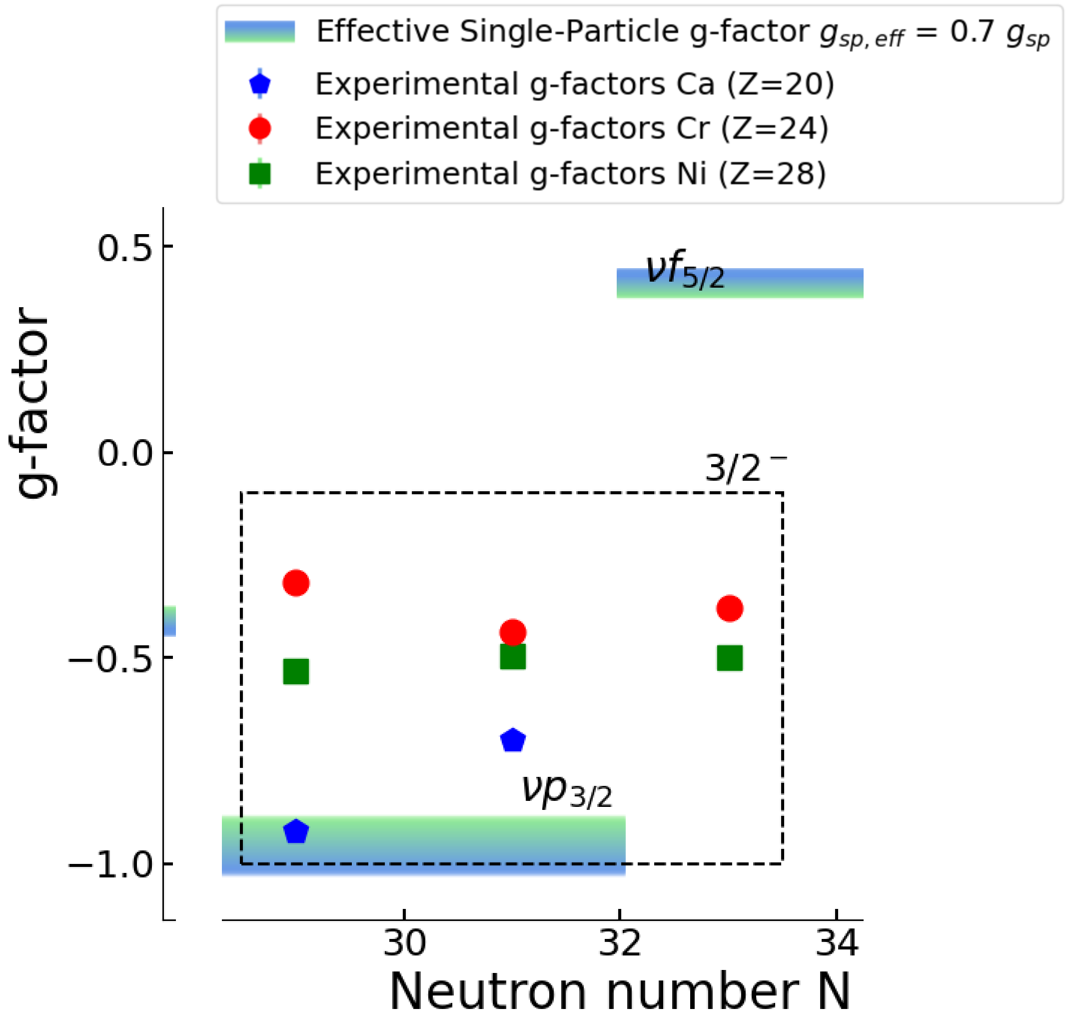

Far from single-particle g-factors

Large amounts of neutron and/or proton excitations, as observed in the Ni isotopes, can be expected.

No solid conclusion can be drawn without further investigation

$^{59,61}Cr$

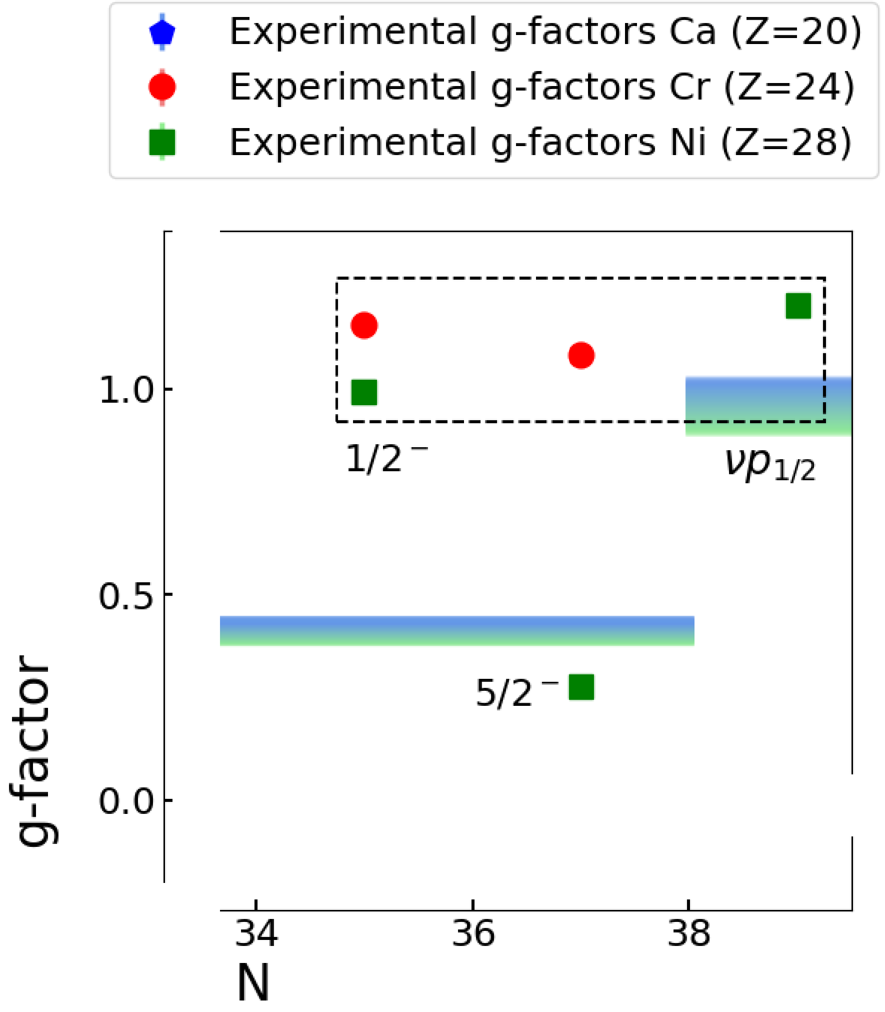

Highly single-particle like behaviour from experimental g-factor and shell model wave function calculations

→ Opposes expected large deformation in this area

Isotope	I^π	Wave function (ν)	GXPF1A Probability	KB3G Probability
^{59}Cr	$1/2^-$	$(1f_{5/2})^2, (1p_{1/2})^1$	**0.63**	**0.60**
^{61}Cr	$1/2^-$	$(1f_{5/2})^4, (1p_{1/2})^1$	**0.76**	**0.75**

S. Suchyta et al. 2014

Conclusion and Outlook

- Unequivocal spin measurements of $^{51-61}\mathrm{Cr}$
- Spin $1/2^{-}$ of $^{61}\mathrm{Cr}$ instead of $5/2^{-}$ from previous measurements.
    - Reinterpretation and remeasurement of β- and γ-decay spectroscopy necessary
- Dipole moments of $^{51-61}\mathrm{Cr}$ measured and compared with corresponding Ca and Ni dipole moments.

➢ Compare dipole moments and spins to calculations, shell model/ab initio

➢ New laser scheme to allow measurement of quadrupole moments

➢ Interpret the measured charge radii of $^{50-62}\mathrm{Cr}$

Thank you for listening

^{61}Cr as a Doorway to the $N = 40$ Island of Inversion

L. Lalanne,[1,2,3,*] M. Athanasakis-Kaklamanakis,[1,2] D.D. Dao,[3] Á. Koszorús,[1] Y. C. Liu,[4] R. Mancheva,[2,1] F. Nowacki,[3] J. Reilly,[5] C. Bernerd,[2] K. Chrysalidis,[2] T. E. Cocolios,[1] R. P. de Groote,[1] K. T. Flanagan,[5] R. F. Garcia Ruiz,[6] D. Hanstorp,[7] R. Heinke,[1] M. Heines,[1] P. Lassegues,[1] K. Mack,[5] B. A. Marsh,[2] A. McGlone,[5] K. M. Lynch,[5] G. Neyens,[1] B. van den Borne,[1] R. Van Duyse,[1] X. F. Yang,[4] and J. Wessolek[5,2]

[1] *KU Leuven, Instituut voor Kern- en Stralingsfysica, B-3001 Leuven, Belgium*
[2] *CERN, CH-1211 Geneva 23, Switzerland*
[3] *Université de Strasbourg, CNRS, IPHC UMR 7178, F-67000 Strasbourg, France*
[4] *School of Physics and State Key Laboratory of Nuclear Physics and Technology, Peking University, Beijing 100871, China*
[5] *Department of Physics and Astronomy, The University of Manchester, Manchester M13 9PL, United Kingdom*
[6] *Massachusetts Institute of Technology, Cambridge, MA 02139, USA*
[7] *Department of Physics, University of Gothenburg, SE-412 96 Gothenburg, Sweden*

(Dated: July 25, 2024)

^{61}Cr $\quad N = 37$

L. Gaudefroy et al. 2005

$3/2^-$ spin of $^{61}_{23}$V assuming small quadrupole deformation

Concluded $f_{5/2}$: $5/2^-$ configuration of ^{61}Cr because GT selection rules favor $\pi f_{7/2} \rightarrow \nu f_{5/2}$ transitions

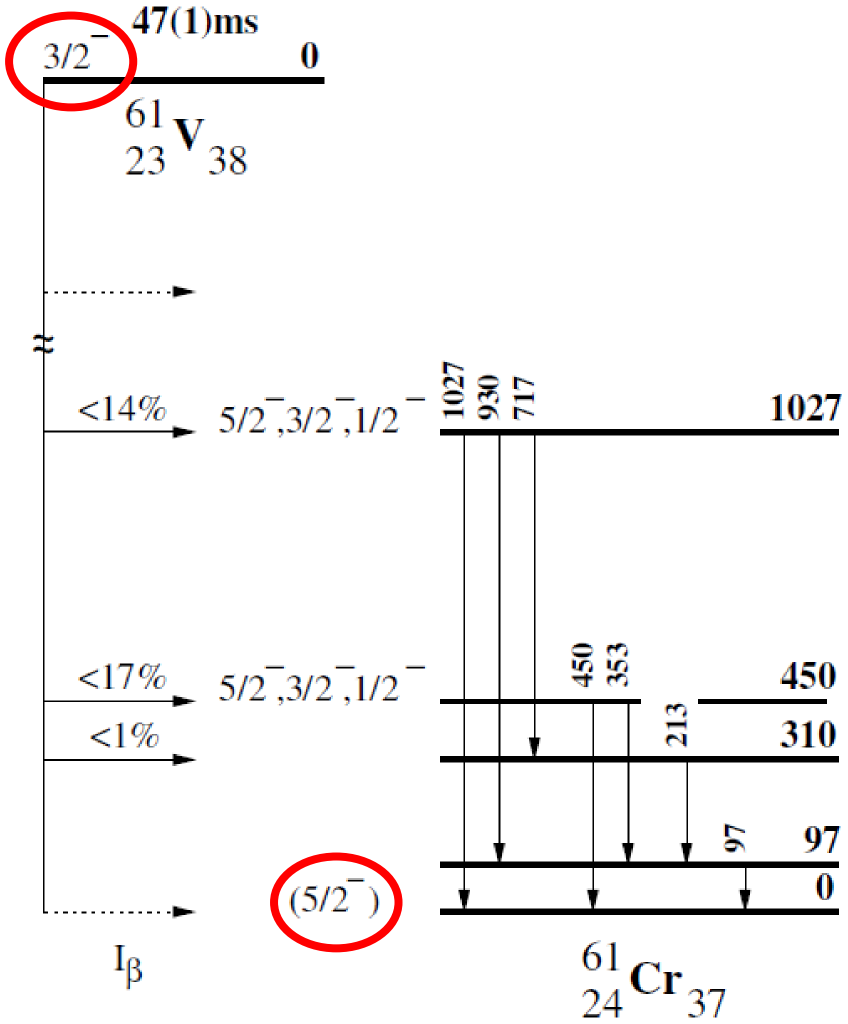

KU LEUVEN

^{61}Cr $\quad N = 37$

S. Suchyta et al. 2014

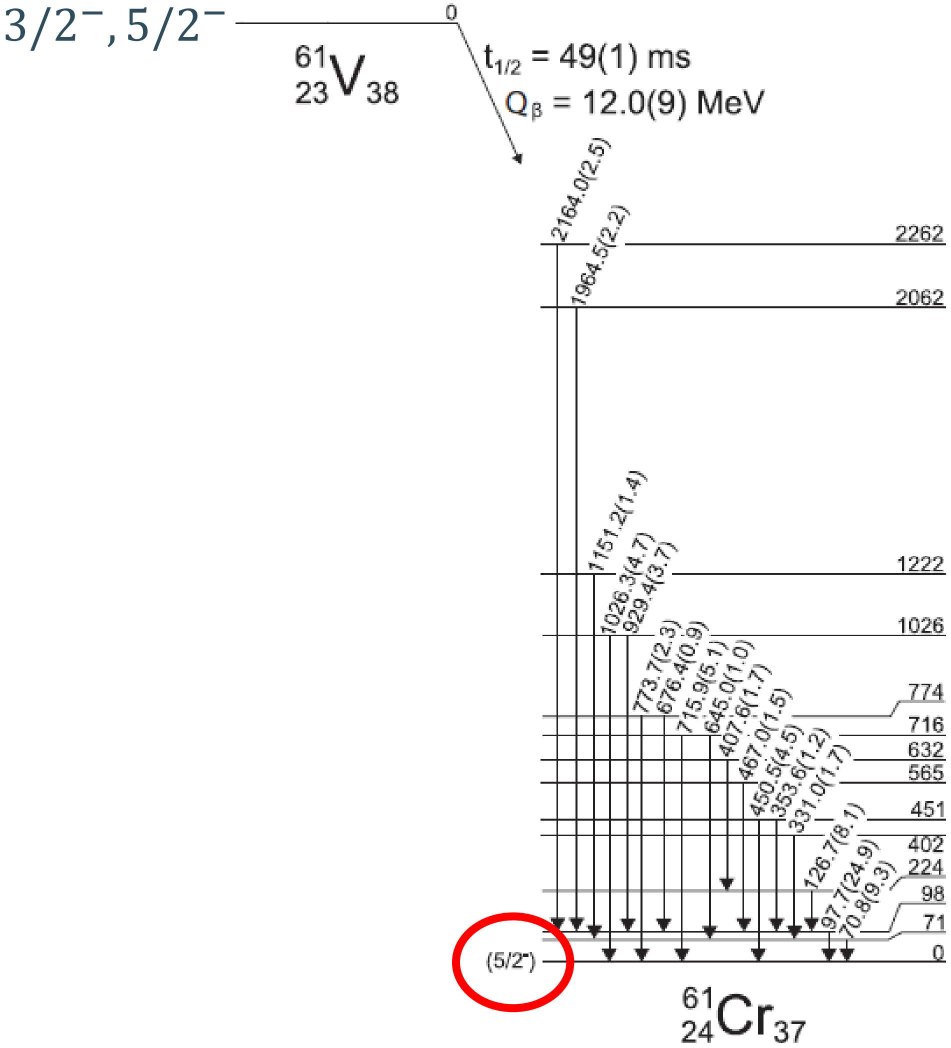

$3/2^-$ spin of $^{61}_{23}V$ most likely for prolate deformation

$5/2^-$ spin of $^{61}_{23}V$ most likely for oblate deformation

S. Suchyta et al. agree with previous spin assignments

But ^{61}Cr $\quad 1/2^-$

$^{51-59}Cr$

All behave as previously measured/predicted

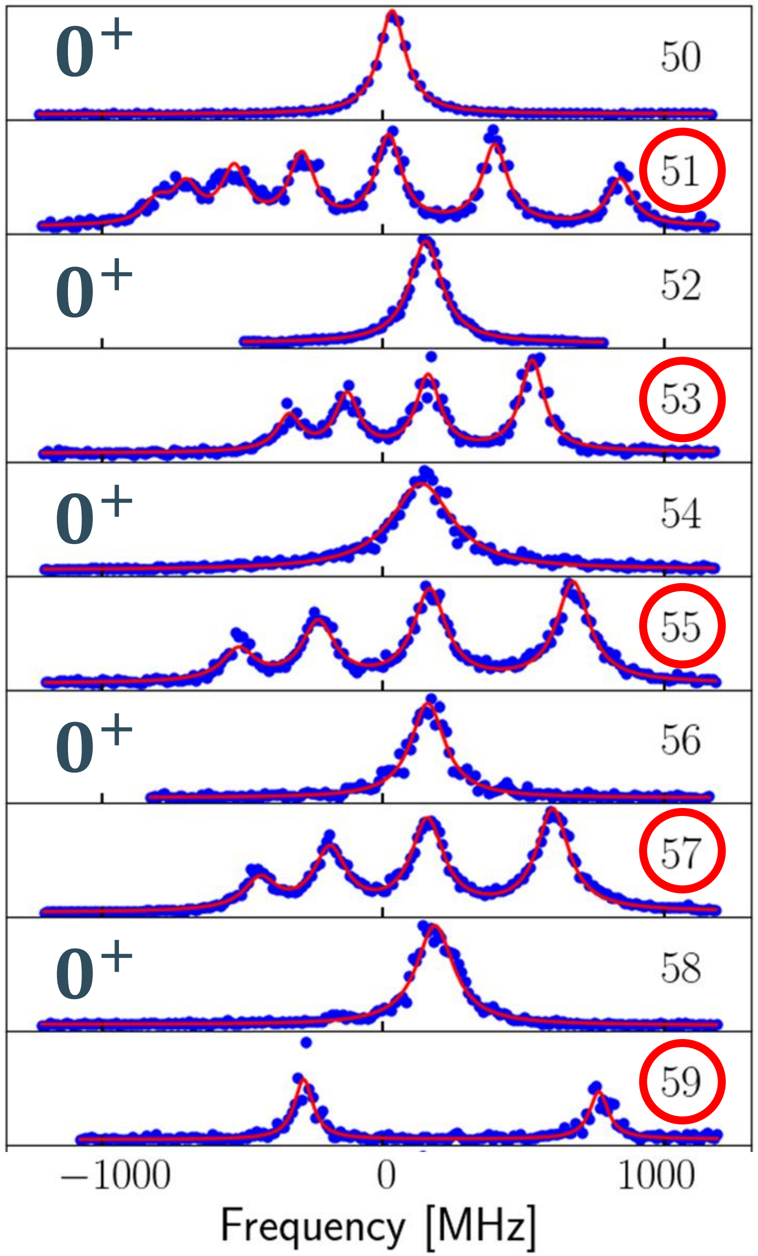

	I Lit	I CRIS
51	$7/2^-$	$7/2^-$
53	$3/2^-$	$3/2^-$
55	$3/2^-$	$3/2^-$
57	$(3/2)^-$	$3/2^-$
59	$(1/2)^-$	$1/2^-$

Folded Yukawa SP level schemes

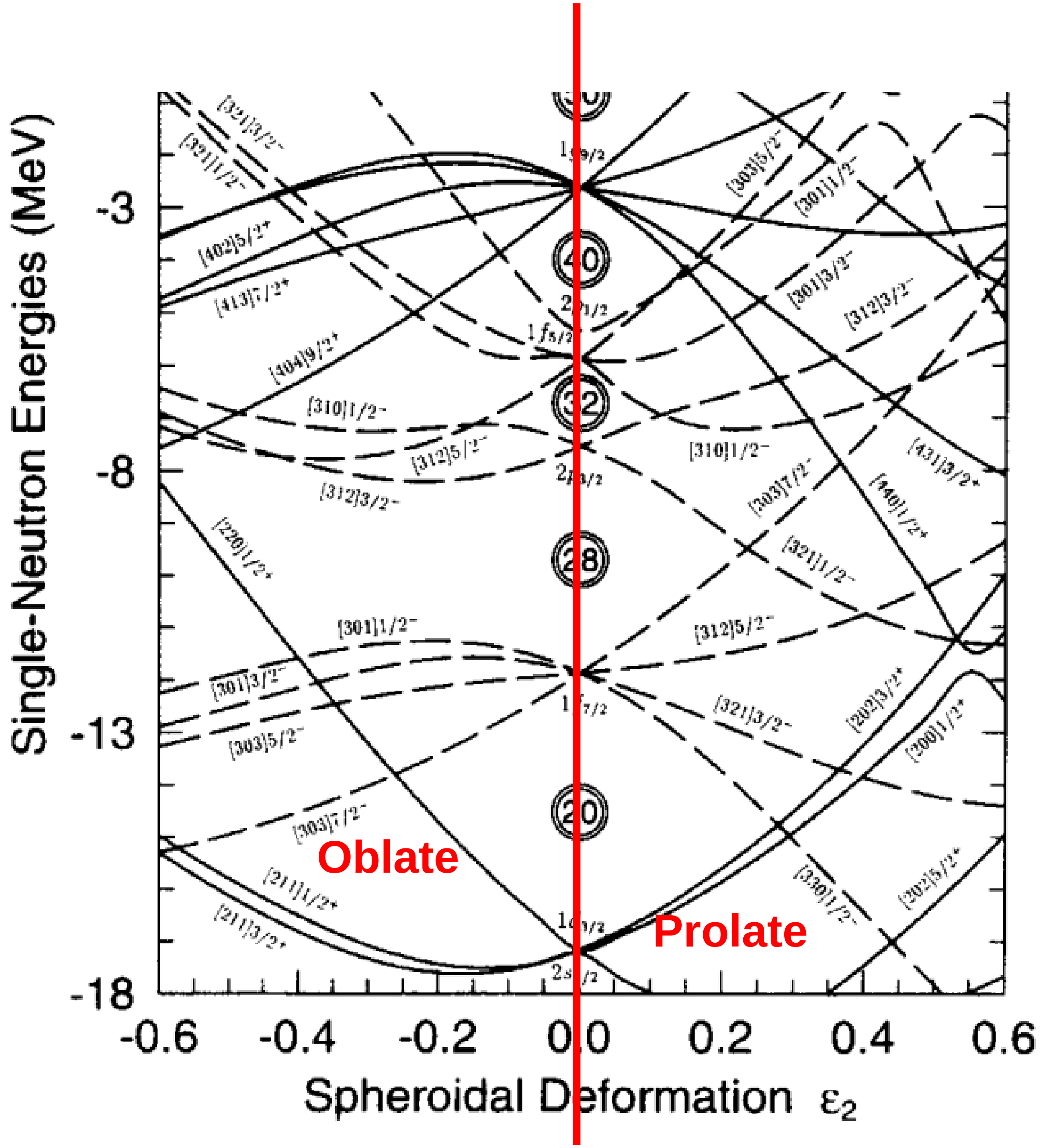

O. Sorlin et al. 1998

Literature and CRIS values of I

51, 53, 55 behave as expected, both according to naive orbital filling and compared to literature

55 → N=31, clearly after N=32 (filling the $\nu p_{3/2}$ orbital) less SP like behaviour.

61 = Star of the experiment, wrong spin assignment in multiple published results.

Unnuanced SP suggestions

5/2

5/2

5/2

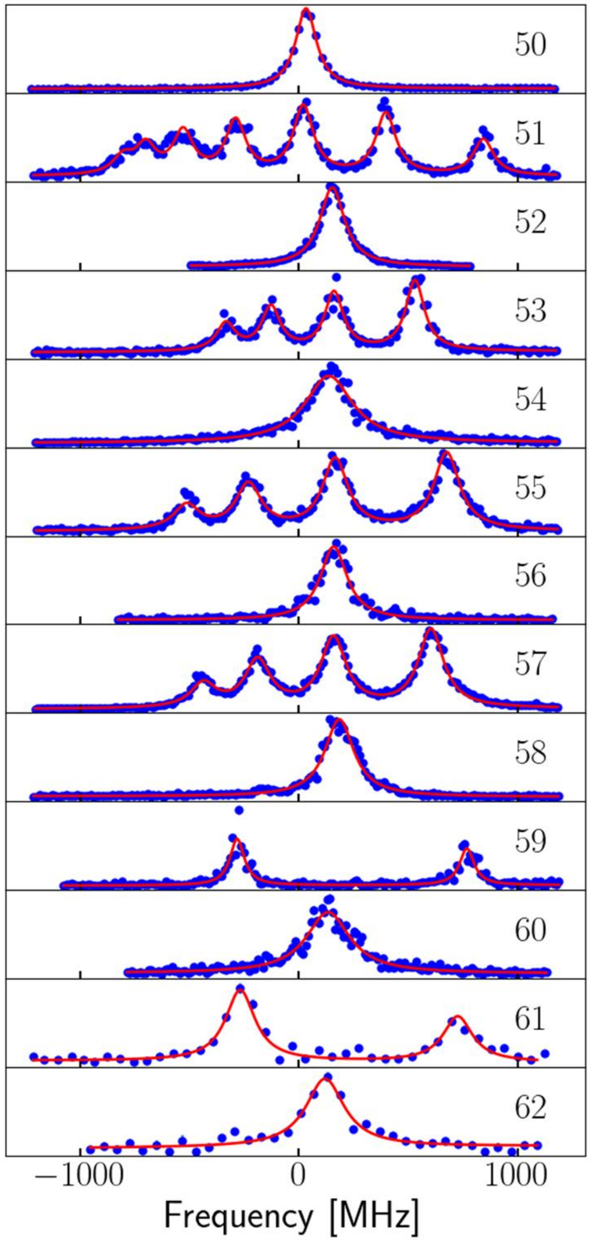

I Lit	I CRIS
$7/2^-$	$7/2^-$
$3/2^-$	$3/2^-$
$3/2^-$	$3/2^-$
$(3/2)^-$	$3/2^-$
$(1/2)^-$	$1/2^-$
$(5/2)^-$	$1/2^-$

Schmidt moments even-odd

$\nu p_{3/2}, \nu f_{7/2} \rightarrow j = l + 1/2$

$\nu p_{1/2}, \nu f_{5/2} \rightarrow j = l - 1/2$

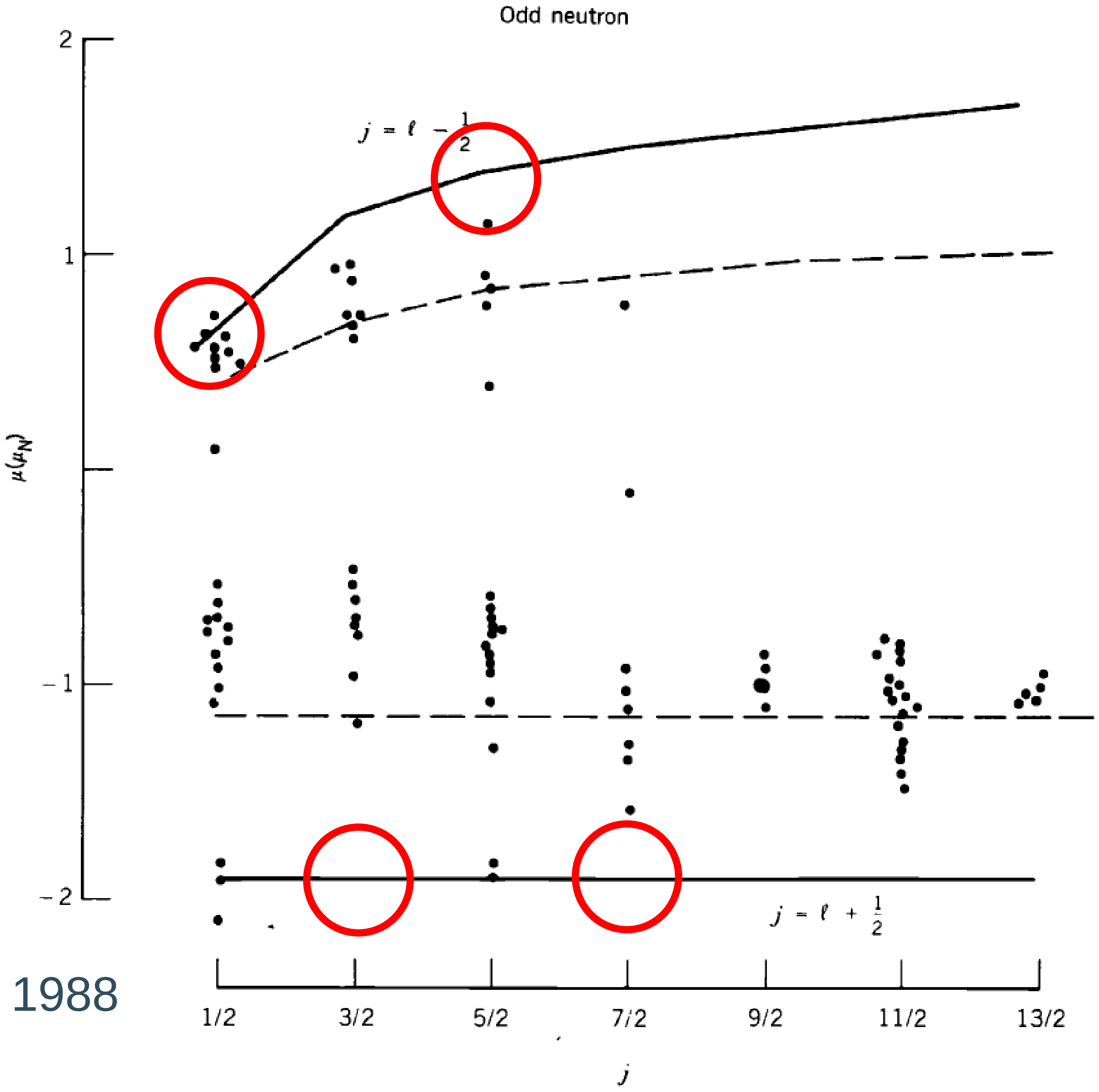

Krane, 1988

KU LEUVEN

Number of peaks simulations

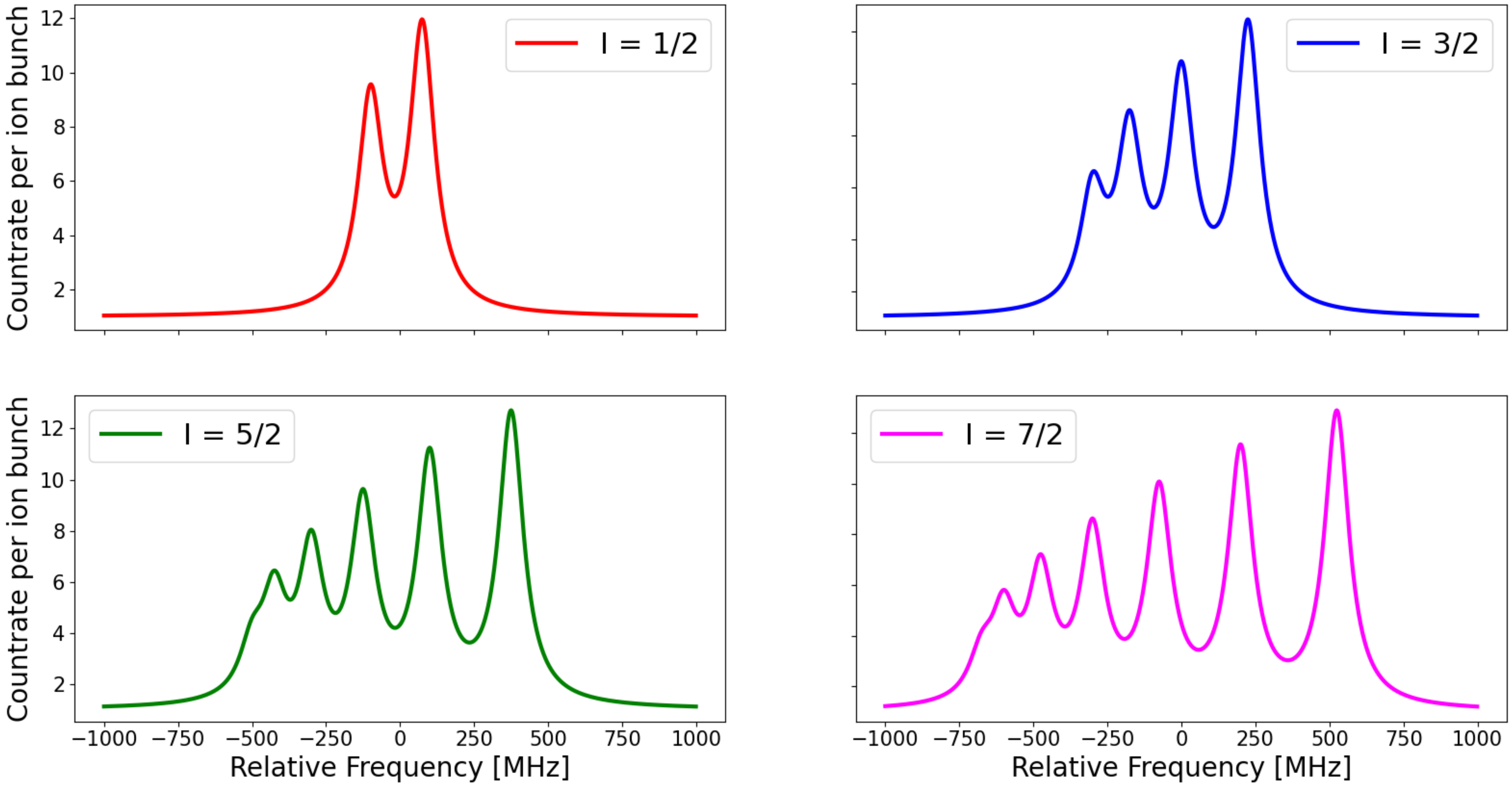

Departement Natuurkunde en Sterrenkunde, Instituut Kern- en Stralingsfysica

KU LEUVEN

Model spaces shell model interactions

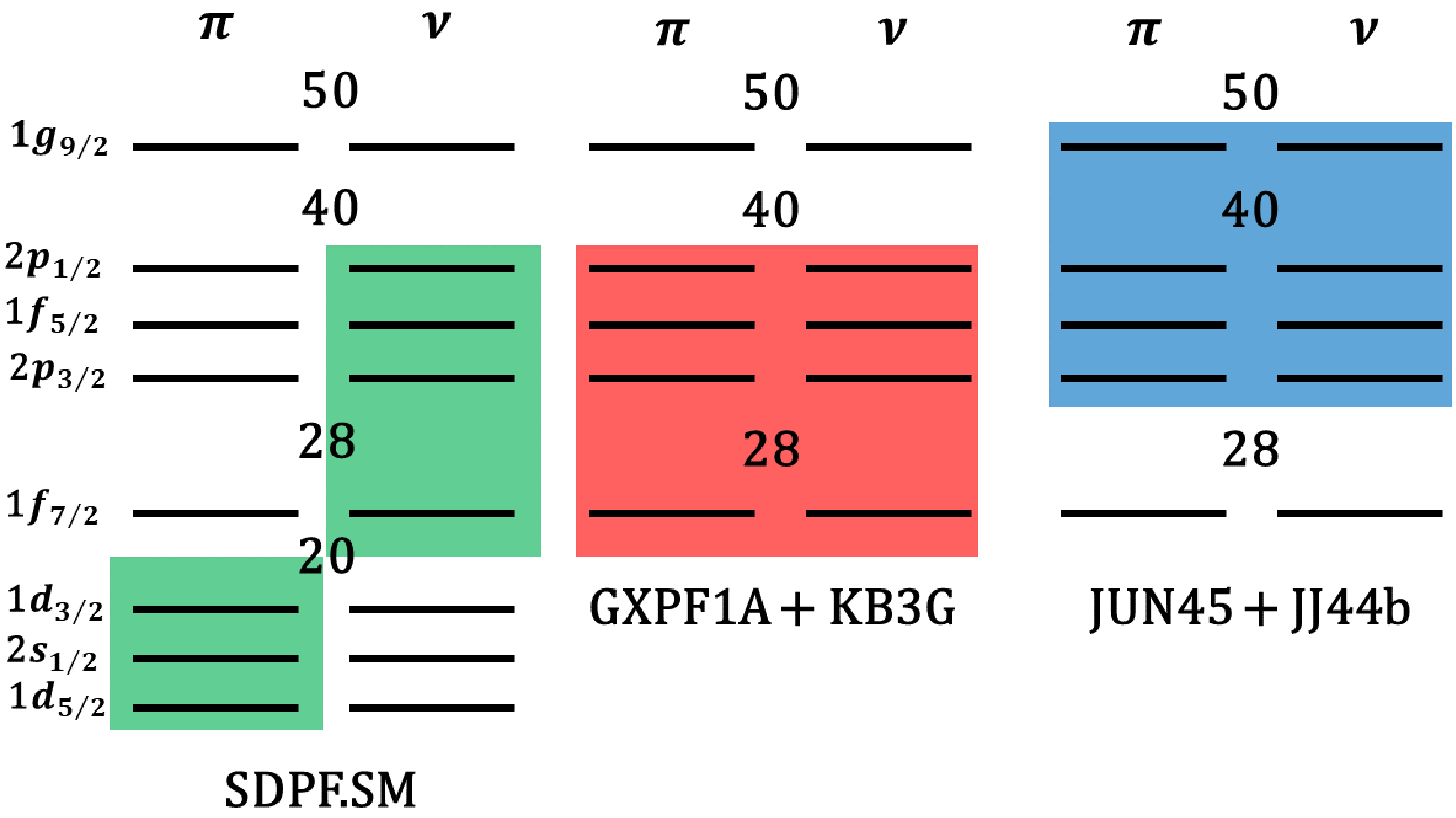

Examples mean and error calculations

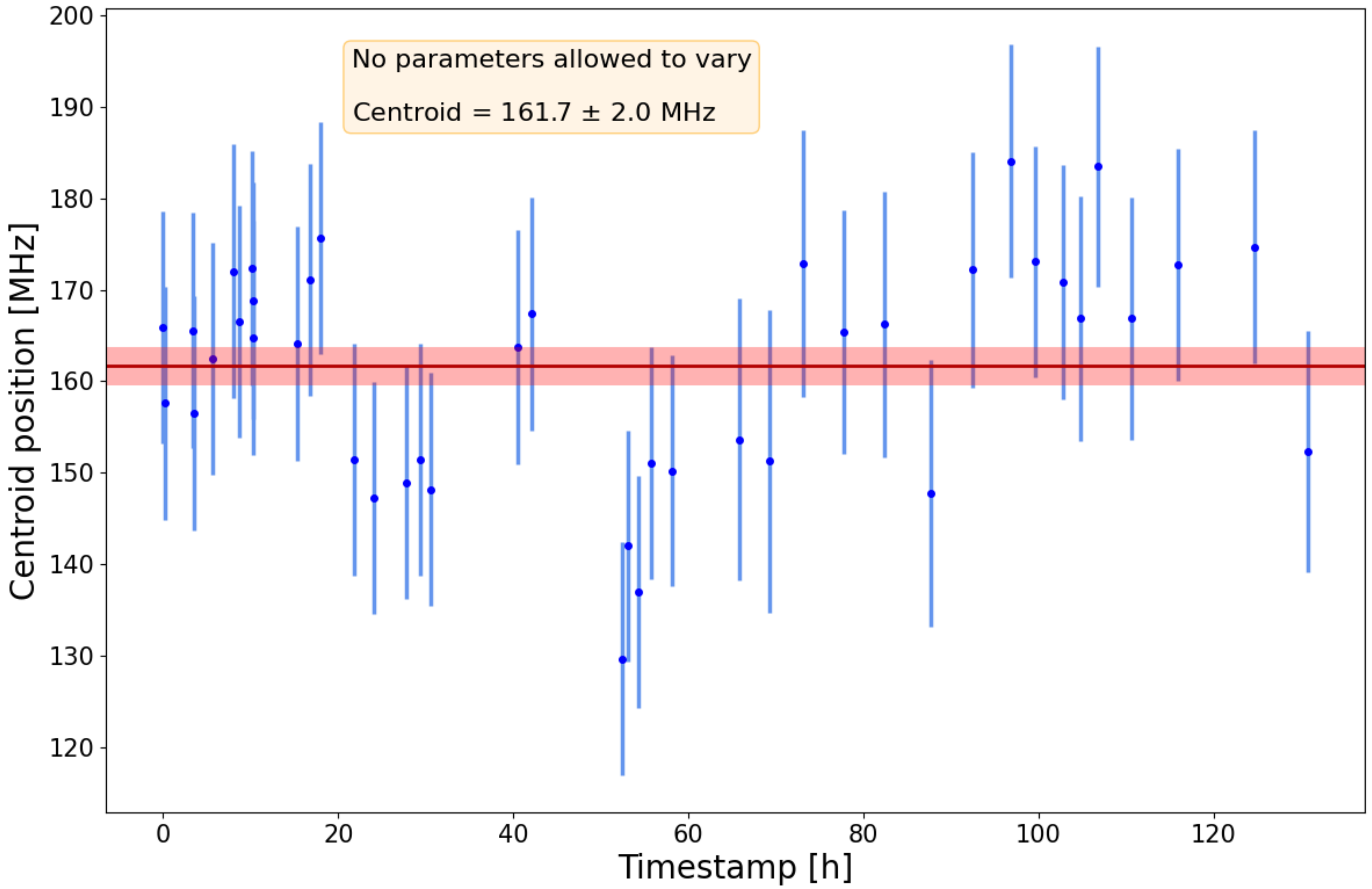

Examples mean and error calculations

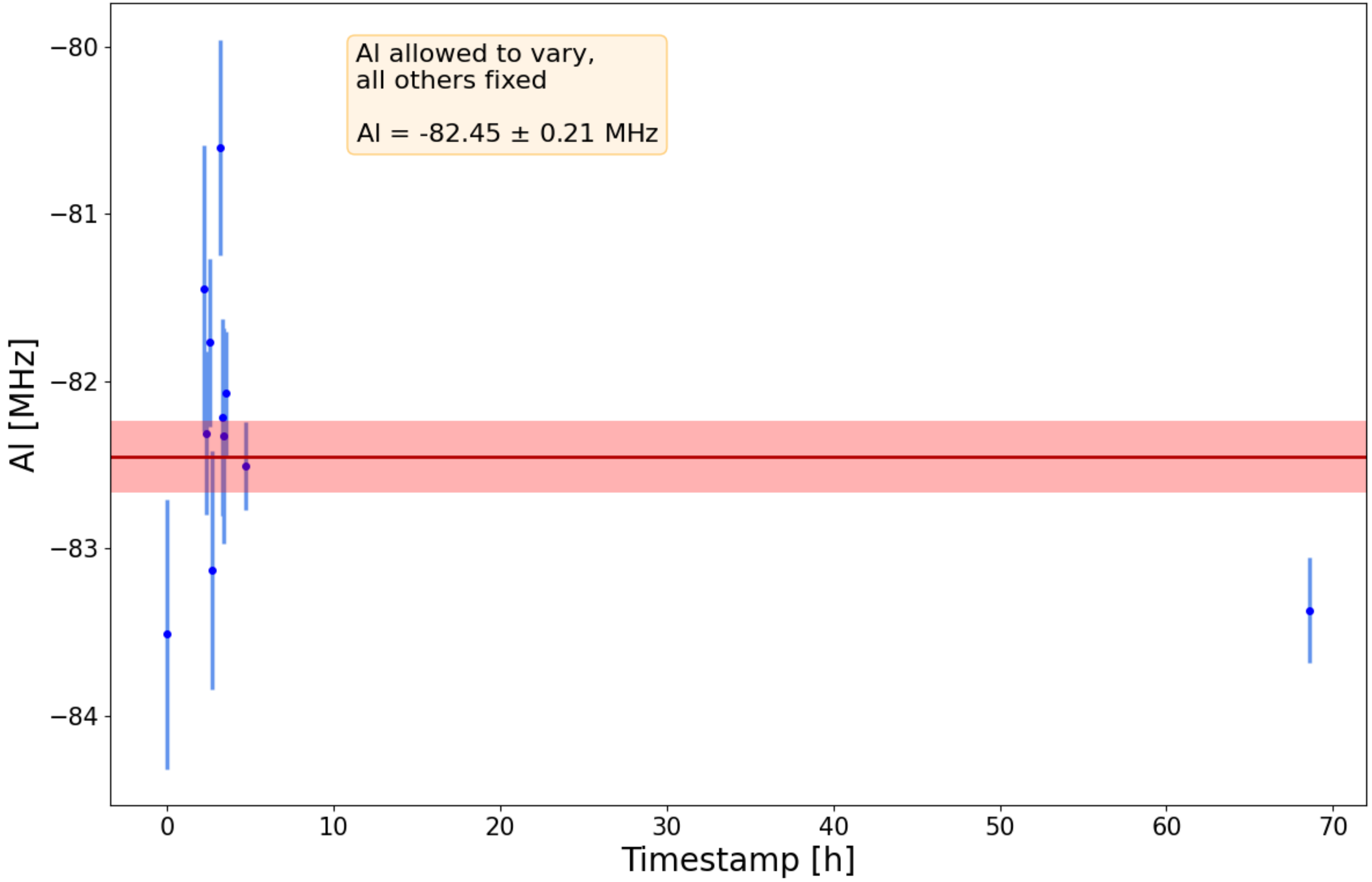

Hyperfine Structure (HFS)

$^{53}\mathrm{Cr}$ $(3/2^{-})$

Spin I	# HF levels
1/2	2
3/2	4
5/2	6
7/2	7

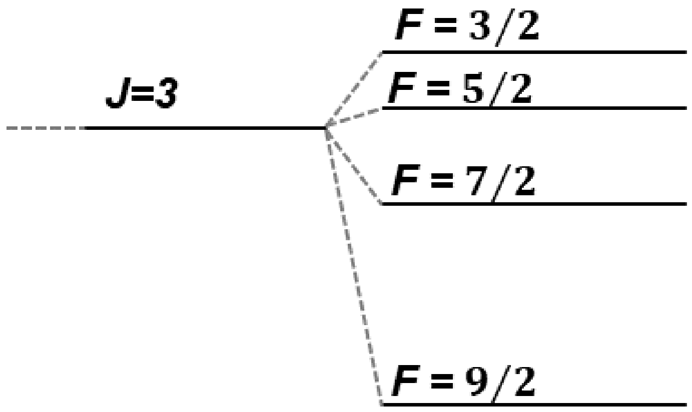

State **HFS**

$\vec{J} = \vec{L} + \vec{S}$ $\vec{F} = \vec{I} + \vec{J}$

The Pandemonium effect

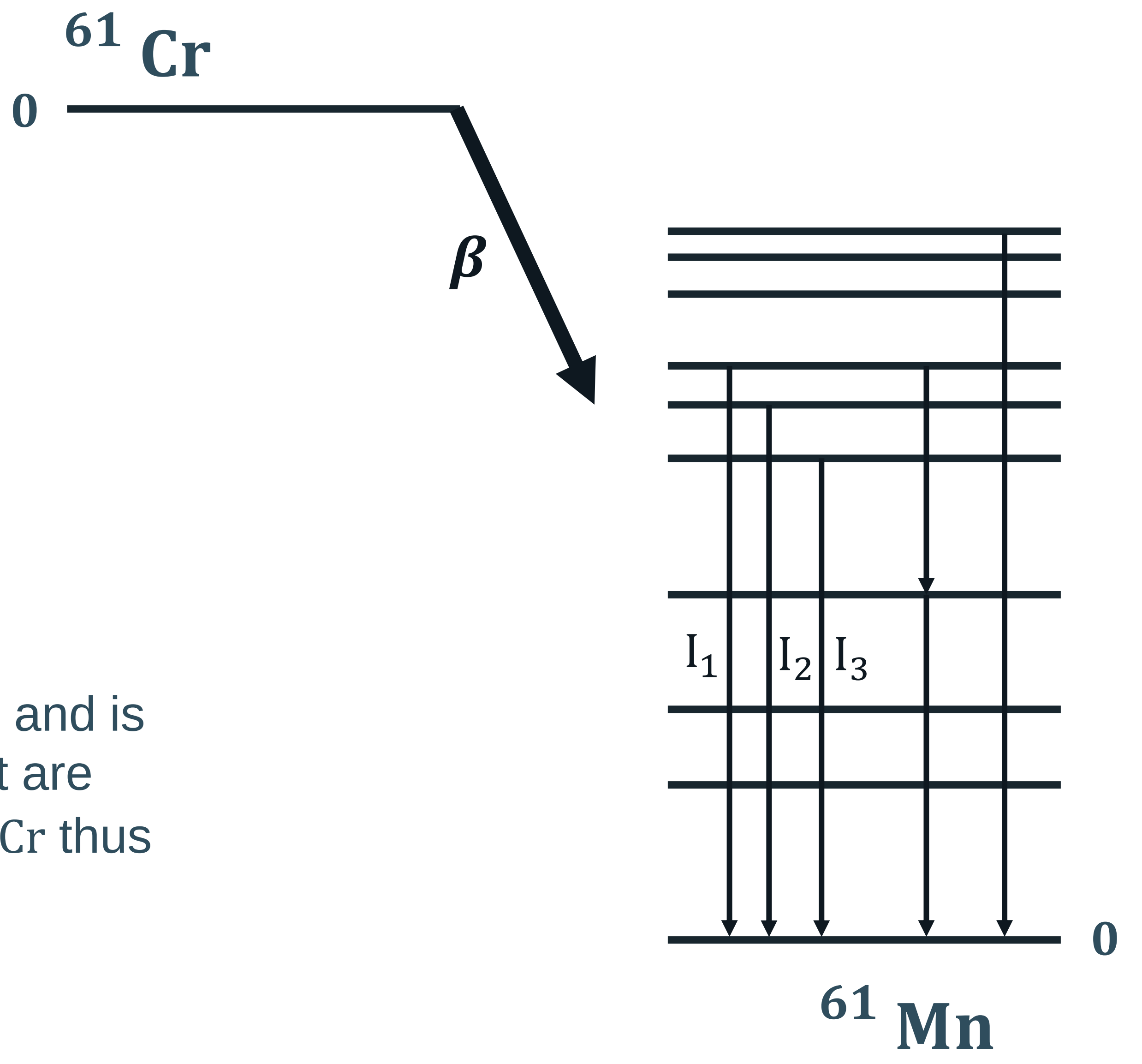

Feeding of the ground state of $^{61}\mathrm{Cr}$

$$F = 100\% - I_1 - I_2 - \ \ldots$$

Assume we observe all gamma rays and is simply not the case. All gammas that are not observed are assigned to GS $^{61}\mathrm{Cr}$ thus overestimating its strength

Nuclear shell structure in Cr

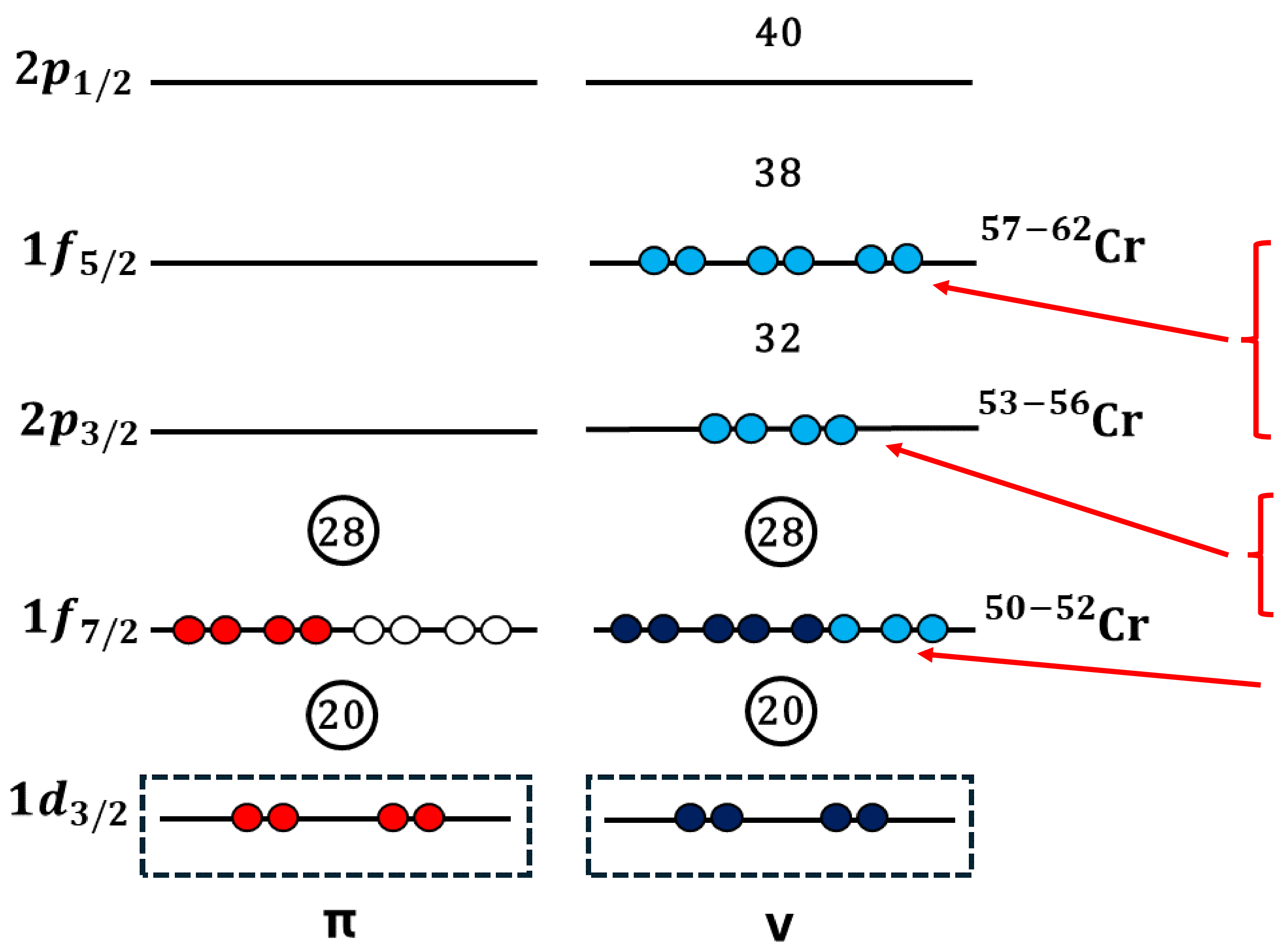

Unnuanced orbital filling and single-particle behaviour

- 61 → 5/2
- 59 → 5/2
- 57 → 5/2
- 55 → 3/2
- 53 → 3/2
- 51 → 7/2

Literature

- 61 → 5/2
- 59 → 5/2
- 57 → 5/2
- 55 → 3/2
- 53 → 3/2
- 51 → 7/2

Departement Natuurkunde en Sterrenkunde, Instituut Kern- en Stralingsfysica

32, 34 neutron shell gaps from mass measurements

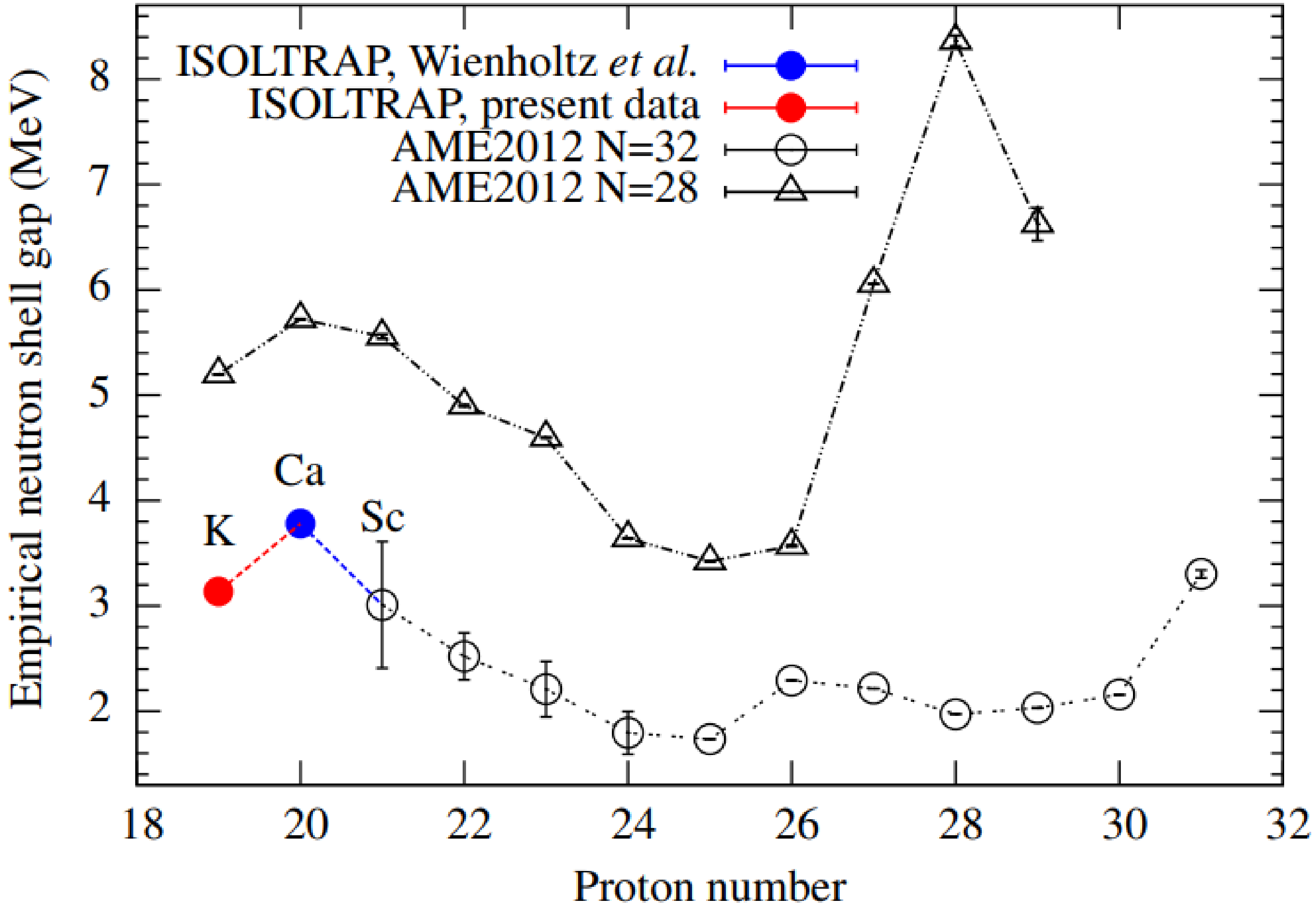

Charge Radii calculation procedure

F = Field shift

K = Mass shift

$$\delta\nu^{AA'} = K\frac{m_{A'} - m_A}{m_{A'}(m_A - m_e)} + F\delta\langle r^2\rangle^{AA'}.$$

$$\mu^{AA'} = \frac{m_{A'} - m_A}{m_{A'}(m_A - m_e)},$$

›e rewritten as

$$\frac{\delta\nu^{AA'}}{\mu^{AA'}} = F\frac{\delta\langle r^2\rangle^{AA'}}{\mu^{AA'}} + K.$$

$$x^{AA'} = \frac{\delta\langle r^2\rangle^{AA'}}{\mu^{AA'}} \quad \& \quad y^{AA'} = \frac{\delta\nu^{AA'}}{\mu^{AA'}},$$

ıd mass shift K can be calculated as

$$F = \frac{x^{50,54} - x^{50,52}}{y^{50,54} - y^{50,52}} \quad \& \quad K = y^{50,54} - Fx^{50,54}.$$

ıd K with their respective errors are shown in equati

$$\mathrm{F} = -266(48)\mathrm{MHz/fm^2} \quad \& \quad \mathrm{K} = -109(12)\mathrm{GHz\ u}$$

King Plot

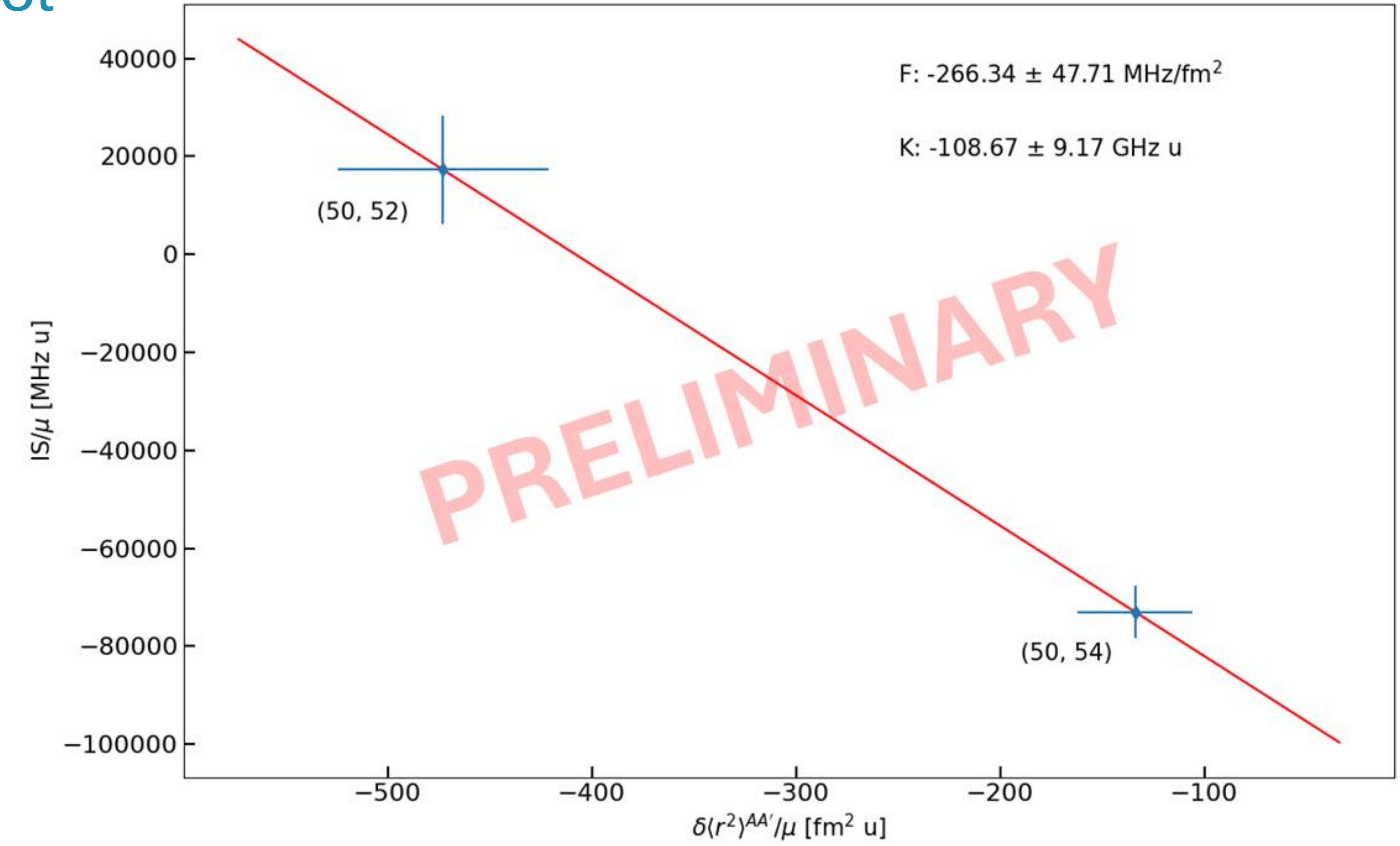

F: -266.34 ± 47.71 MHz/fm^2
K: -108.67 ± 9.17 GHz u
(50, 52)
(50, 54)
PRELIMINARY
40000
20000
0
−20000
−40000
−60000
−80000
−100000
IS/μ [MHz u]
−500
−400
−300
−200
−100
$\delta\langle r^2\rangle^{AA'}/\mu$ [fm^2 u]

Charge Radii

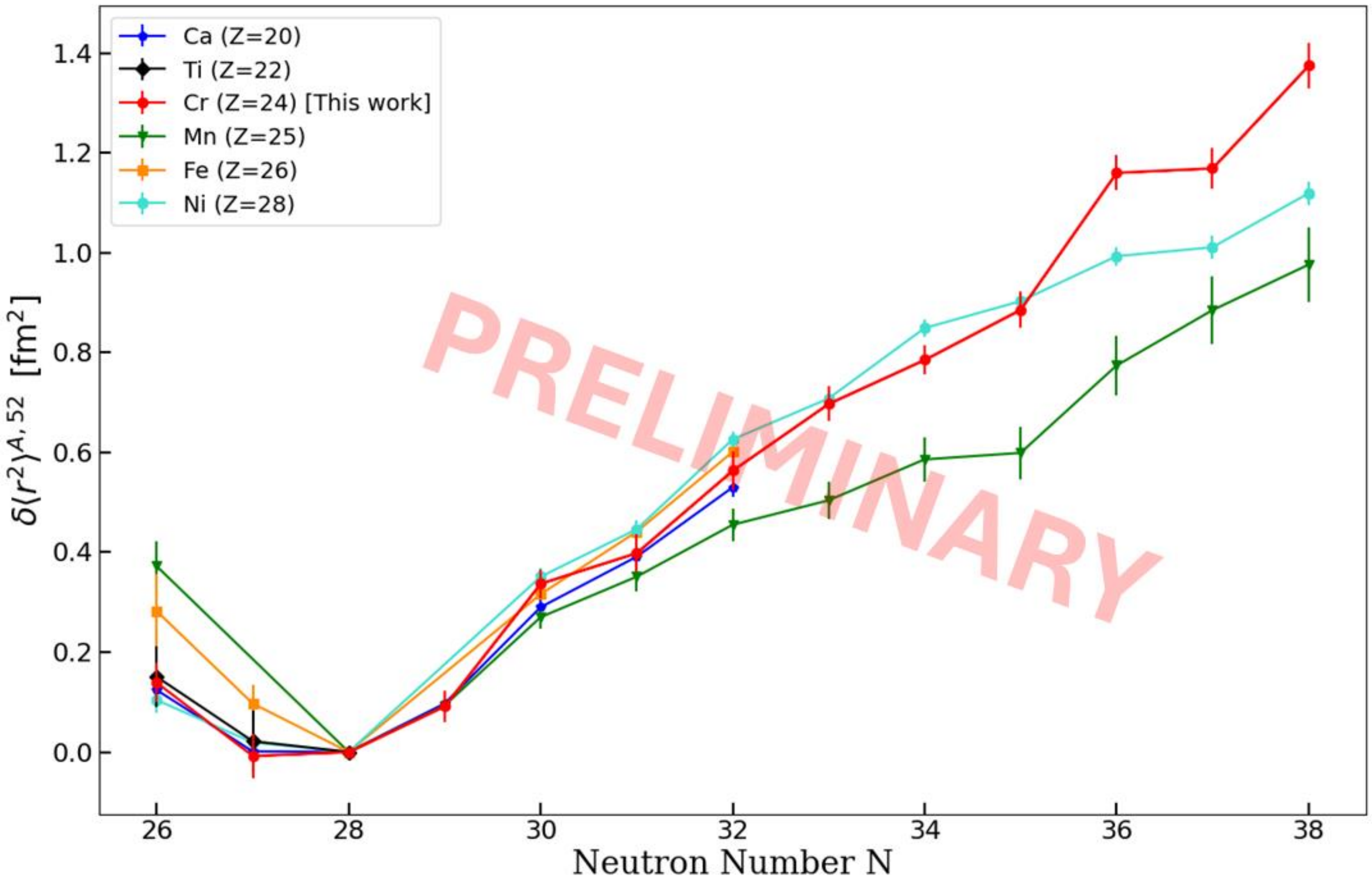

Shell structure evolution from Ca to Ni

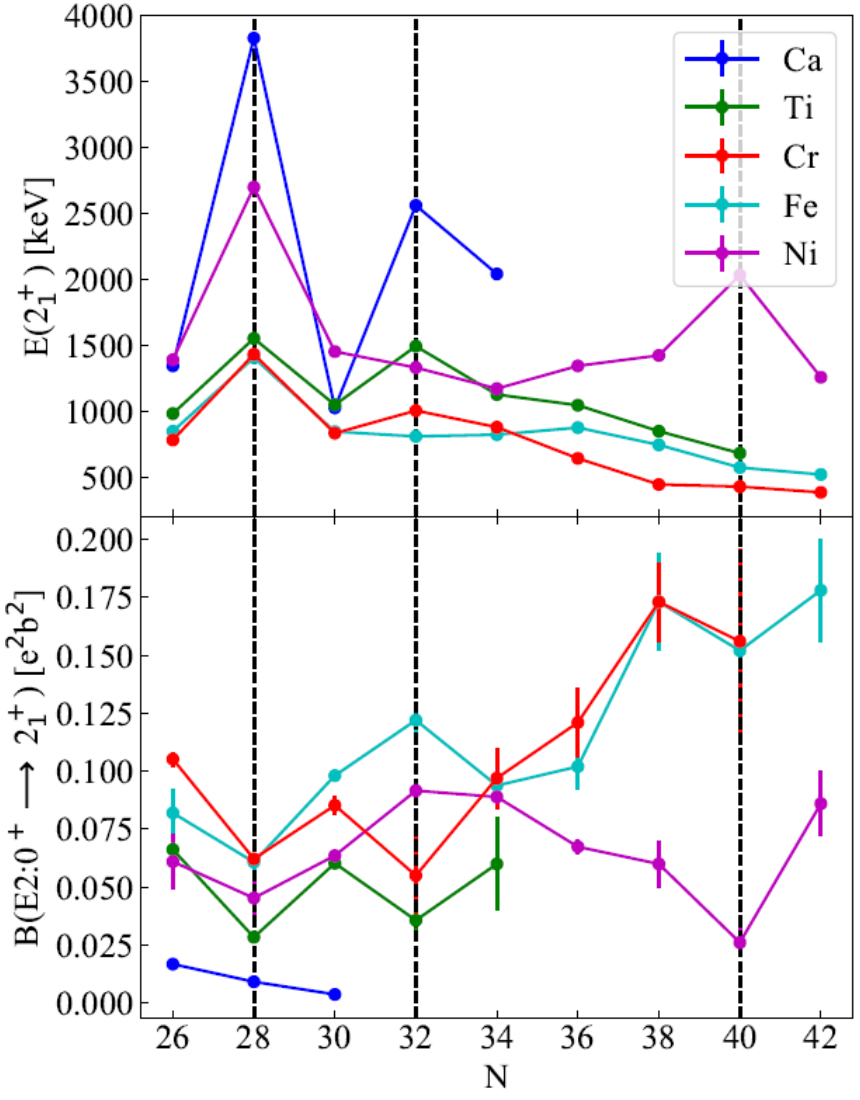

Towards *N*=40

Low E(2_1^+) in Cr and Fe, compared to Ni

High B(E2: 0^+ → 2_1^+) in Cr and Fe, not in Ni

Collective behaviour and deformation expected in Cr going towards *N*=40

Figure taken from L. Lalanne, A. Koszorús, M. Athanasakis-Kaklamanakis, et al., “Collinear resonance ionization spectroscopy of chromium isotopes between N = 28 and N= 40,” Tech. Rep., May 2022. [Online]. Available: https://cds.cern.ch/record/2809064

Observables to investigate

Nuclear ground State Spin *I*

even-even → 0^+

even-odd → depends on specific configuration of neutrons

RMS Charge Radius $<r_c^2>$

Expect small radii for stable nuclei = around magic numbers

Large radii for deformed nuclei

Nuclear magnetic dipole moment *μ*

$$\mu = g I \mu_N .$$

Interaction of nucleus with magnetic fields

g-factor sensitive to specific configuration

Nuclear electric quadrupole moment *Q*

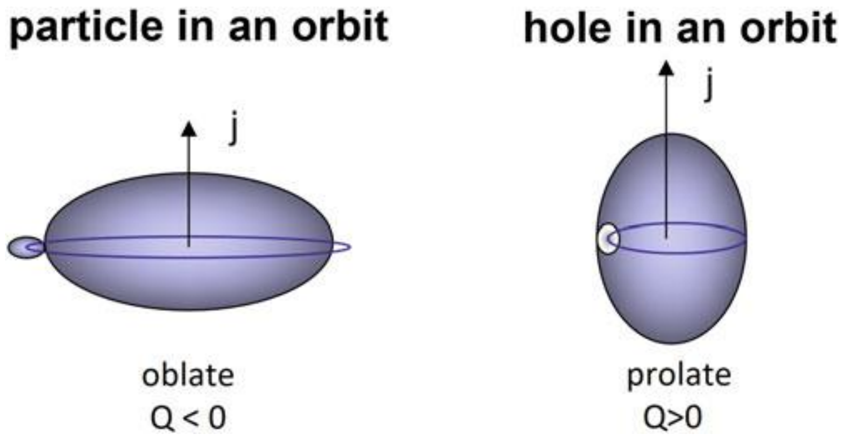

Figure taken from R. P. de Groote and G. Neyens, "Spins and Electromagnetic Moments of Nuclei," in Handbook of Nuclear Physics, Springer Nature Singapore, 2022, pp. 1–36. doi: 10.1007/978-981-15-8818-1{_}42-1

Observables to investigate

Nuclear ground State Spin *I*

even-even → 0^+

even-odd → depends on specific configuration of neutrons orbitals

Nuclear magnetic dipole moment *μ*

even-even → 0^+

even-odd → depends on specific configuration of neutrons orbitals

Interaction of nucleus with magnetic fields

g-factor sensitive to specific configuration

RMS Charge Radius $<r_c^2>$

Further interpretation necessary

Nuclear electric quadrupole moment *Q*

For Cr impossible to measure within experimental resolution (~ 100 MHz)

Nuclear shell structure in Cr

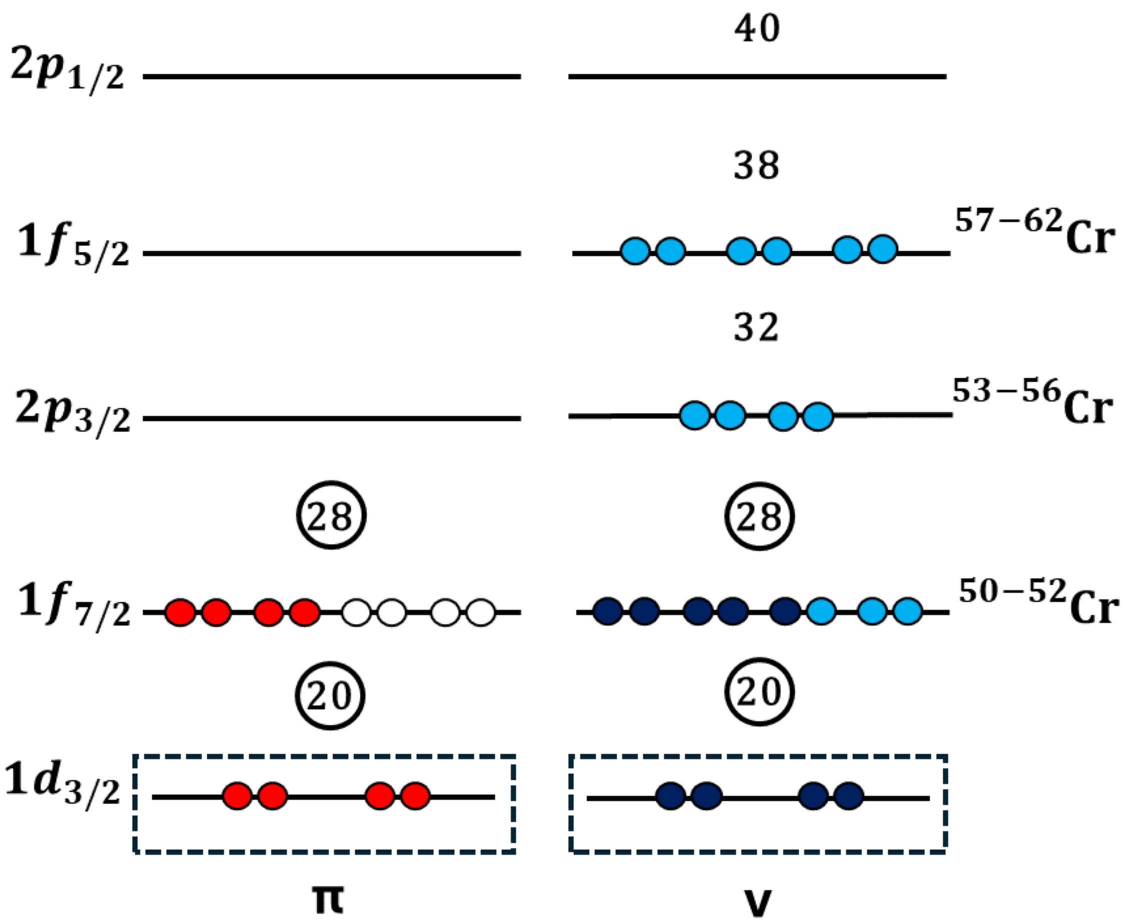

Unnuanced orbital filling and single-particle behaviour

- 51 → 7/2
- 53 → 3/2
- 55 → 3/2
- 57 → 5/2
- 59 → 5/2
- 61 → 5/2

Literature

- 51 → $7/2^-$ measured
- 53 → $3/2^-$ measured
- 55 → $3/2^-$ measured
- 57 → $3/2^-$ tentative
- 59 → $1/2^-$ tentative
- 61 → $5/2^-$ tentative

Isotope	J^π	GXPF1A Wave function (neutron)	Probability	KB3G Wave function (neutron)	Probability
^{55}Cr	$1/2^-_1$	$(0f_{7/2})^8,(1p_{3/2})^2,(0f_{5/2})^1,(1p_{1/2})^0$	0.24	$(0f_{7/2})^8,(1p_{3/2})^2,(0f_{5/2})^1,(1p_{1/2})^0$	0.26
		$(0f_{7/2})^8,(1p_{3/2})^2,(0f_{5/2})^0,(1p_{1/2})^1$	0.22	$(0f_{7/2})^8,(1p_{3/2})^1,(0f_{5/2})^1,(1p_{1/2})^1$	0.18
		$(0f_{7/2})^8,(1p_{3/2})^1,(0f_{5/2})^1,(1p_{1/2})^1$	0.16	$(0f_{7/2})^8,(1p_{3/2})^2,(0f_{5/2})^0,(1p_{1/2})^1$	0.14
	$3/2^-_1$	$(0f_{7/2})^8,(1p_{3/2})^3,(0f_{5/2})^0,(1p_{1/2})^0$	0.47	$(0f_{7/2})^8,(1p_{3/2})^3,(0f_{5/2})^0,(1p_{1/2})^0$	0.37
		$(0f_{7/2})^8,(1p_{3/2})^2,(0f_{5/2})^0,(1p_{1/2})^1$	0.11		
	$5/2^-_1$	$(0f_{7/2})^8,(1p_{3/2})^2,(0f_{5/2})^1,(1p_{1/2})^0$	0.44	$(0f_{7/2})^8,(1p_{3/2})^2,(0f_{5/2})^1,(1p_{1/2})^0$	0.42
		$(0f_{7/2})^8,(1p_{3/2})^1,(0f_{5/2})^1,(1p_{1/2})^1$	0.10		
^{57}Cr	$1/2^-_1$	$(0f_{7/2})^8,(1p_{3/2})^4,(0f_{5/2})^0,(1p_{1/2})^1$	0.51	$(0f_{7/2})^8,(1p_{3/2})^4,(0f_{5/2})^0,(1p_{1/2})^1$	0.19
		$(0f_{7/2})^8,(1p_{3/2})^2,(0f_{5/2})^2,(1p_{1/2})^1$	0.12	$(0f_{7/2})^8,(1p_{3/2})^4,(0f_{5/2})^1,(1p_{1/2})^0$	0.18
				$(0f_{7/2})^8,(1p_{3/2})^3,(0f_{5/2})^2,(1p_{1/2})^0$	0.14
				$(0f_{7/2})^8,(1p_{3/2})^3,(0f_{5/2})^1,(1p_{1/2})^1$	0.10
	$3/2^-_1$	$(0f_{7/2})^8,(1p_{3/2})^3,(0f_{5/2})^2,(1p_{1/2})^0$	0.39	$(0f_{7/2})^8,(1p_{3/2})^3,(0f_{5/2})^2,(1p_{1/2})^0$	0.47
		$(0f_{7/2})^8,(1p_{3/2})^3,(0f_{5/2})^1,(1p_{1/2})^1$	0.12		
	$5/2^-_1$	$(0f_{7/2})^8,(1p_{3/2})^4,(0f_{5/2})^1,(1p_{1/2})^0$	0.45	$(0f_{7/2})^8,(1p_{3/2})^4,(0f_{5/2})^1,(1p_{1/2})^0$	0.38
		$(0f_{7/2})^8,(1p_{3/2})^3,(0f_{5/2})^1,(1p_{1/2})^1$	0.15	$(0f_{7/2})^8,(1p_{3/2})^3,(0f_{5/2})^1,(1p_{1/2})^1$	0.15
				$(0f_{7/2})^8,(1p_{3/2})^2,(0f_{5/2})^1,(1p_{1/2})^2$	0.10
^{59}Cr	$1/2^-_1$	$(0f_{7/2})^8,(1p_{3/2})^4,(0f_{5/2})^2,(1p_{1/2})^1$	0.63	$(0f_{7/2})^8,(1p_{3/2})^4,(0f_{5/2})^2,(1p_{1/2})^1$	0.60
	$3/2^-_1$	$(0f_{7/2})^8,(1p_{3/2})^4,(0f_{5/2})^2,(1p_{1/2})^1$	0.44	$(0f_{7/2})^8,(1p_{3/2})^4,(0f_{5/2})^3,(1p_{1/2})^0$	0.36
		$(0f_{7/2})^8,(1p_{3/2})^4,(0f_{5/2})^3,(1p_{1/2})^0$	0.12	$(0f_{7/2})^8,(1p_{3/2})^4,(0f_{5/2})^2,(1p_{1/2})^1$	0.22
		$(0f_{7/2})^8,(1p_{3/2})^3,(0f_{5/2})^2,(1p_{1/2})^2$	0.11		
	$5/2^-_1$	$(0f_{7/2})^8,(1p_{3/2})^4,(0f_{5/2})^1,(1p_{1/2})^2$	0.28	$(0f_{7/2})^8,(1p_{3/2})^4,(0f_{5/2})^3,(1p_{1/2})^0$	0.47
		$(0f_{7/2})^8,(1p_{3/2})^4,(0f_{5/2})^3,(1p_{1/2})^0$	0.21	$(0f_{7/2})^8,(1p_{3/2})^3,(0f_{5/2})^3,(1p_{1/2})^1$	0.11
		$(0f_{7/2})^8,(1p_{3/2})^4,(0f_{5/2})^2,(1p_{1/2})^1$	0.15	$(0f_{7/2})^8,(1p_{3/2})^2,(0f_{5/2})^3,(1p_{1/2})^2$	0.10
^{61}Cr	$1/2^-_1$	$(0f_{7/2})^8,(1p_{3/2})^4,(0f_{5/2})^4,(1p_{1/2})^1$	0.76	$(0f_{7/2})^8,(1p_{3/2})^4,(0f_{5/2})^4,(1p_{1/2})^1$	0.75
	$3/2^-_1$	$(0f_{7/2})^8,(1p_{3/2})^4,(0f_{5/2})^3,(1p_{1/2})^2$	0.71	$(0f_{7/2})^8,(1p_{3/2})^4,(0f_{5/2})^4,(1p_{1/2})^1$	0.44
		$(0f_{7/2})^8,(1p_{3/2})^4,(0f_{5/2})^4,(1p_{1/2})^1$	0.13	$(0f_{7/2})^8,(1p_{3/2})^4,(0f_{5/2})^3,(1p_{1/2})^2$	0.33
	$5/2^-_1$	$(0f_{7/2})^8,(1p_{3/2})^4,(0f_{5/2})^3,(1p_{1/2})^2$	0.78	$(0f_{7/2})^8,(1p_{3/2})^4,(0f_{5/2})^3,(1p_{1/2})^2$	0.60
				$(0f_{7/2})^8,(1p_{3/2})^4,(0f_{5/2})^4,(1p_{1/2})^1$	0.10

S. Suchyta et al. 2014

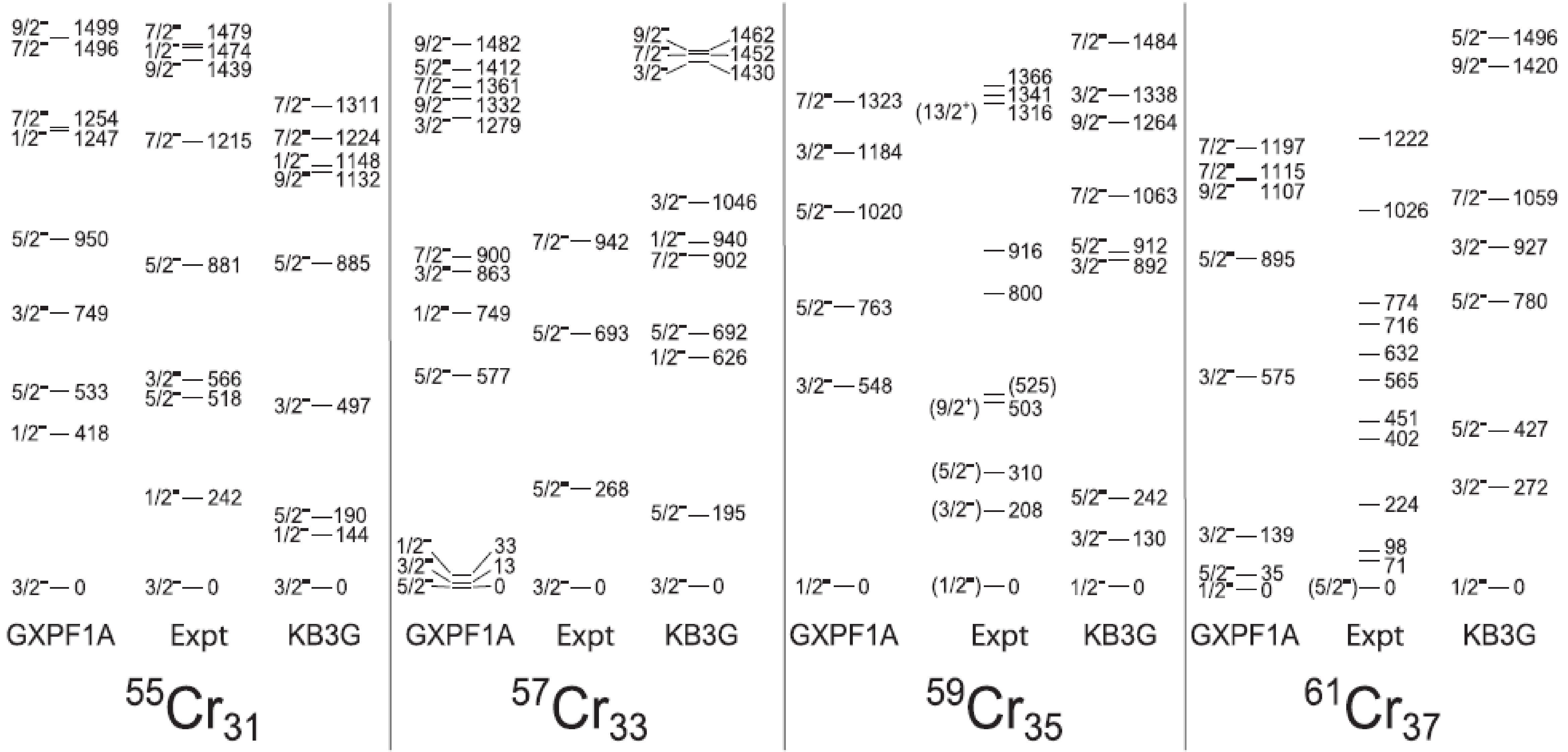

S. Suchyta et al. 2014

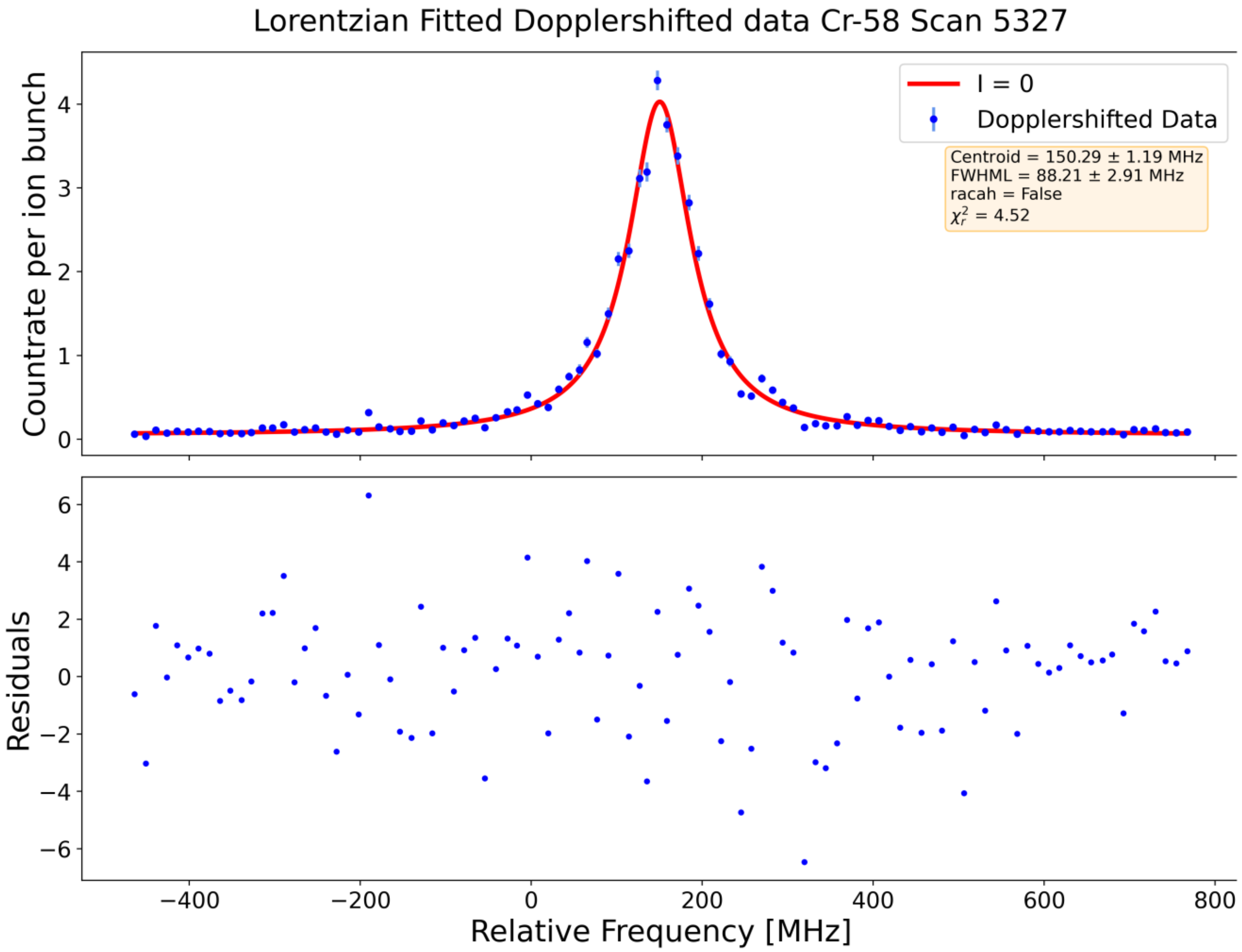
Lorentzian Fitted Dopplershifted data Cr-58 Scan 5327
I = 0
Dopplershifted Data
Centroid = 150.29 ± 1.19 MHz
FWHML = 88.21 ± 2.91 MHz
racah = False
χ_r^2 = 4.52
Countrate per ion bunch
Residuals
Relative Frequency [MHz]

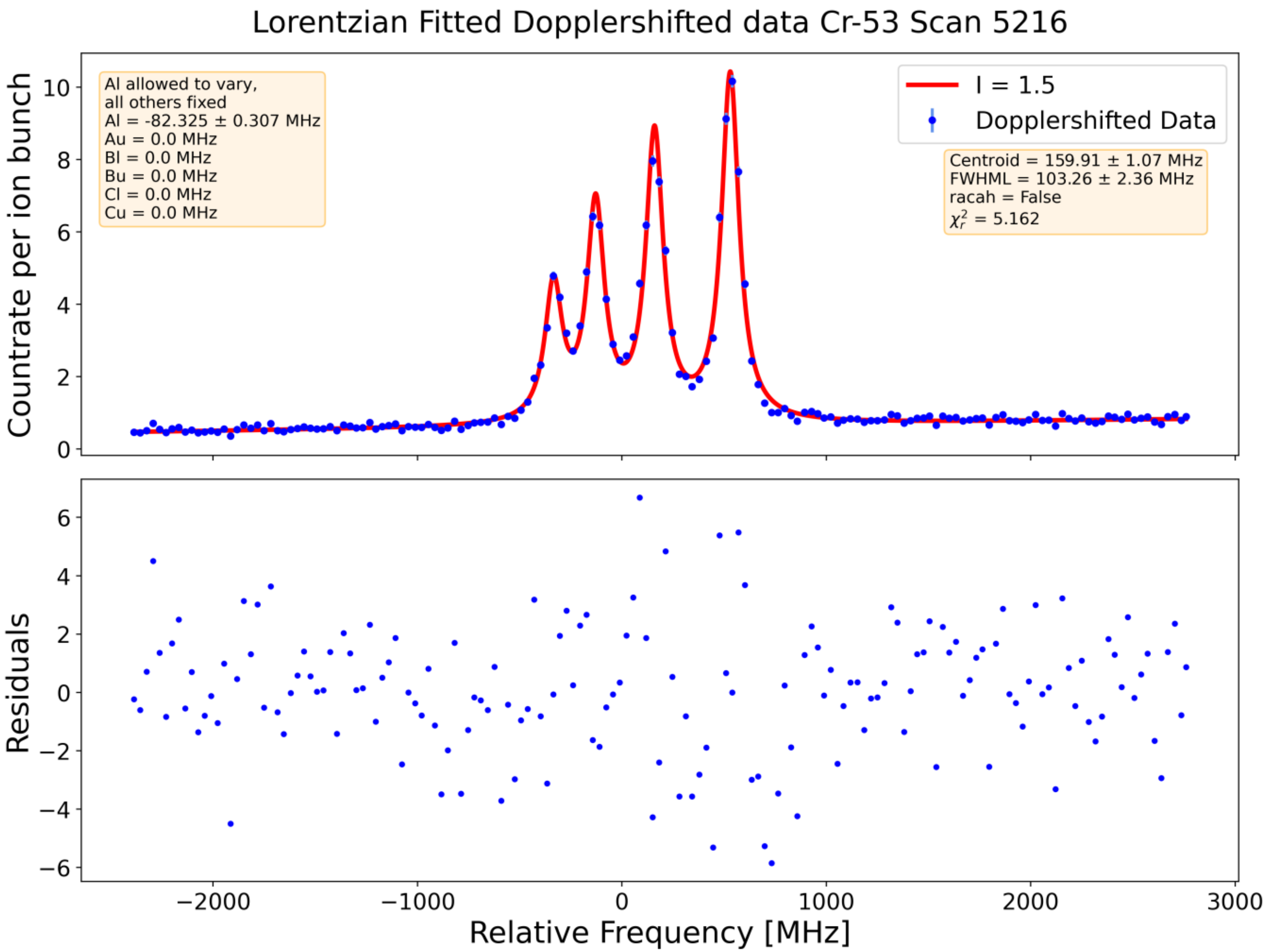
Lorentzian Fitted Dopplershifted data Cr-53 Scan 5216
Al allowed to vary,
all others fixed
Al = -82.325 ± 0.307 MHz
Au = 0.0 MHz
Bl = 0.0 MHz
Bu = 0.0 MHz
Cl = 0.0 MHz
Cu = 0.0 MHz
I = 1.5
Dopplershifted Data
Centroid = 159.91 ± 1.07 MHz
FWHML = 103.26 ± 2.36 MHz
racah = False
χ_r^2 = 5.162
Countrate per ion bunch
Residuals
Relative Frequency [MHz]

Weighted mean

$$\hat{\mu} = \frac{\sum_{i=1}^{n} x_i w_i}{\sum_{i=1}^{n} w_i}. \qquad w_i = \frac{1}{\sigma_i^2},$$

Std variation of mean

$$\hat{\sigma}_{\hat{\mu}}^2 = \sigma_{\hat{\mu}}^2 \chi^2 = \frac{1}{n-1} \frac{1}{\sum_{i=1}^{n} w_i} \sum_{i=1}^{n} w_i (x_i - \hat{\mu})^2,$$

$$\chi^2 \equiv \frac{1}{n-1} \sum_{i=1}^{n} w_i (x_i - \hat{\mu})^2.$$

Weighted mean

$$\hat{\mu} = \frac{\sum_{i=1}^{n} x_i w_i}{\sum_{i=1}^{n} w_i}. \qquad w_i = \frac{1}{\sigma_i^2},$$

How to calculate the error on each datapoint

Std variation of the ref. isotope

$$\sigma_{tot,i} = \sqrt{\sigma_i^2 + \sigma^2}, \qquad \sigma^2 = \frac{\sum_{i=1}^{n}(x_i - \hat{\mu})^2}{n-1}.$$

Departement Natuurkunde en Sterrenkunde, Instituut Kern- en Stralingsfysica

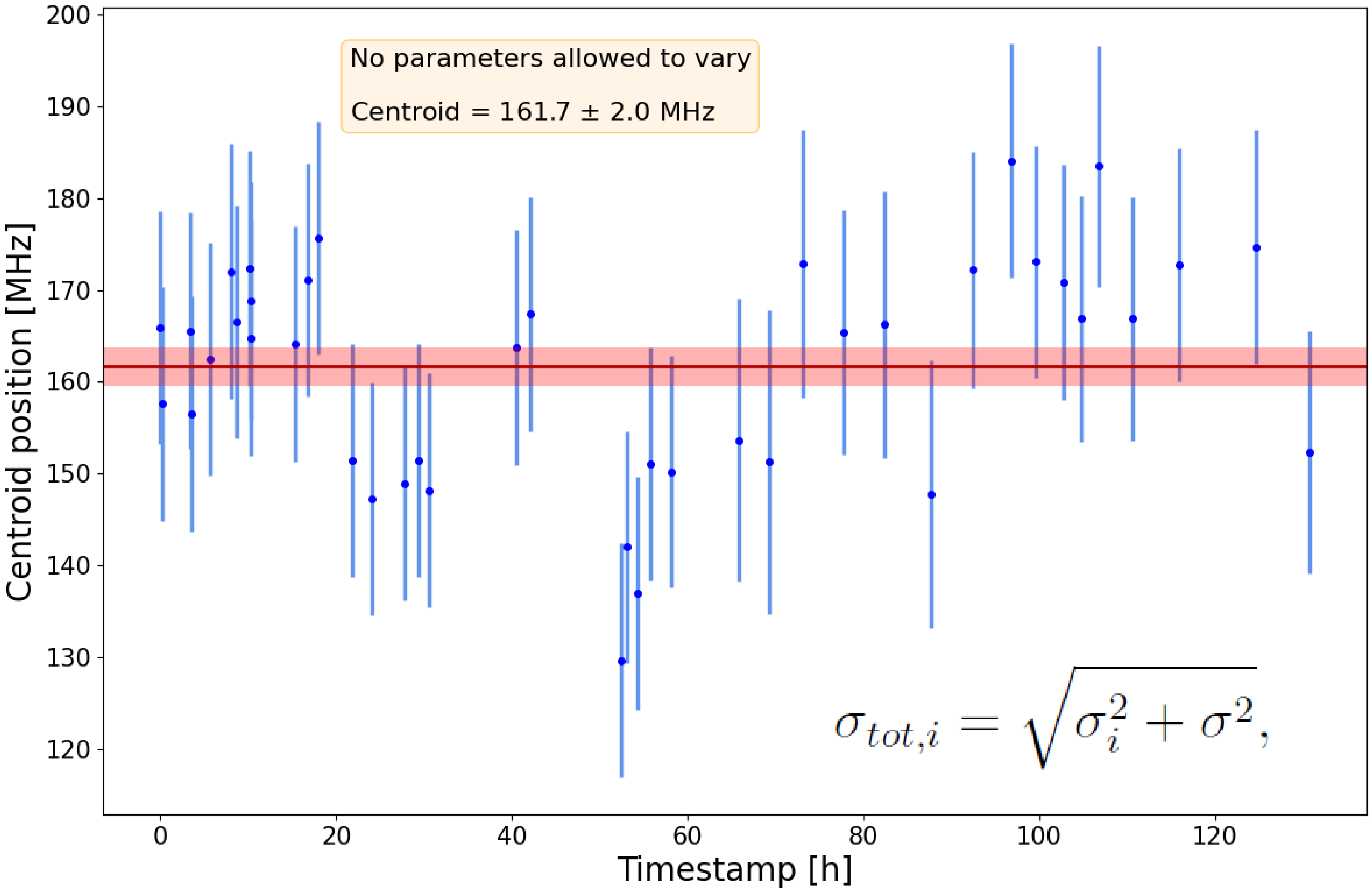

$$\sigma_{tot,i} = \sqrt{\sigma_i^2 + \sigma^2},$$

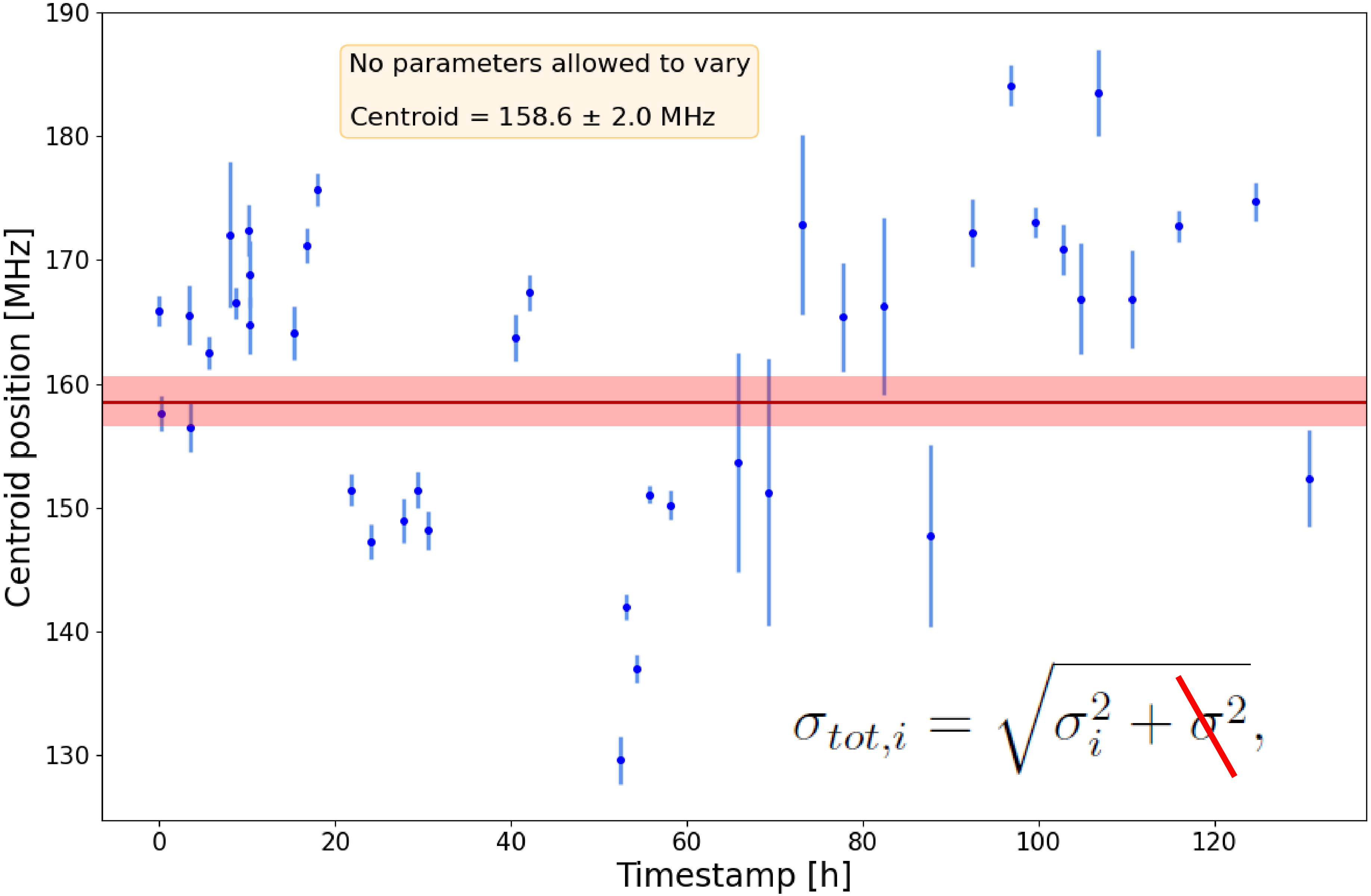
No parameters allowed to vary
Centroid = 158.6 ± 2.0 MHz
190
180
170
160
150
140
130
Centroid position [MHz]
0
20
40
60
80
100
120
Timestamp [h]
$\sigma_{tot,i} = \sqrt{\sigma_i^2 + \sigma^2},$

Last option: add σ to final error on weighted mean → Very large errors

$$\sigma_{tot,i} = \sqrt{\sigma_i^2 + \sigma^2},$$

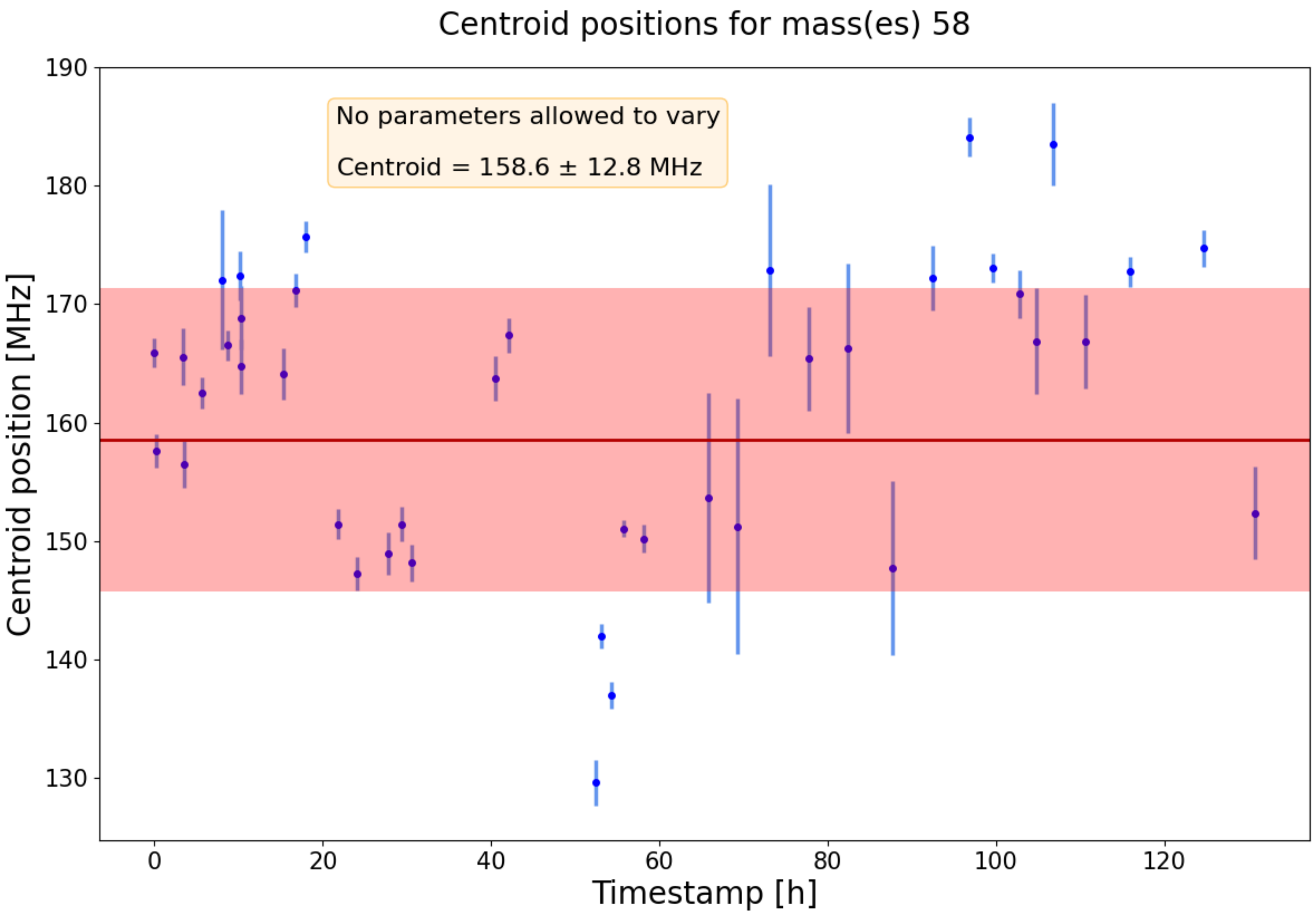

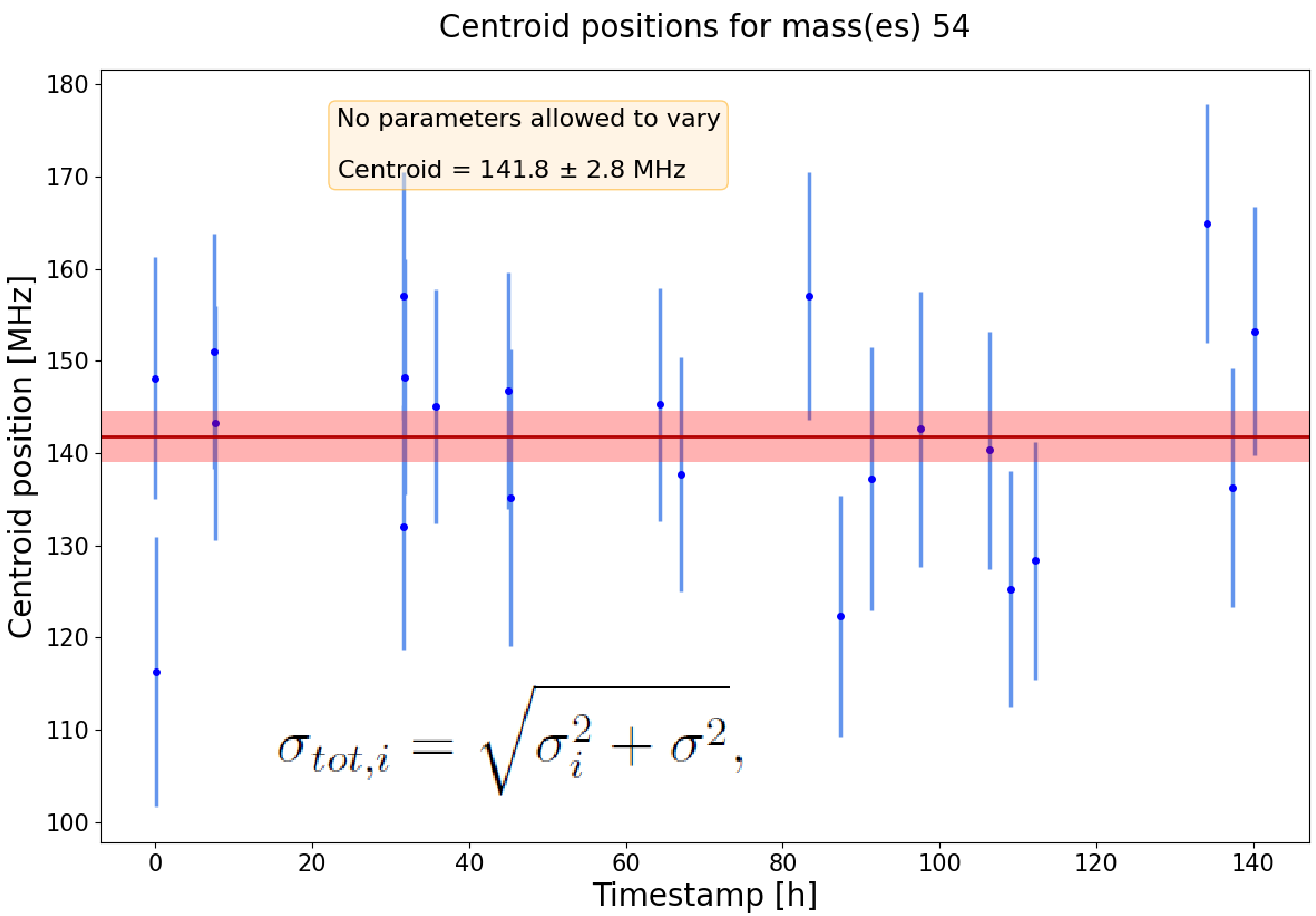

$$\sigma_{tot,i} = \sqrt{\sigma_i^2 + \sigma^2},$$

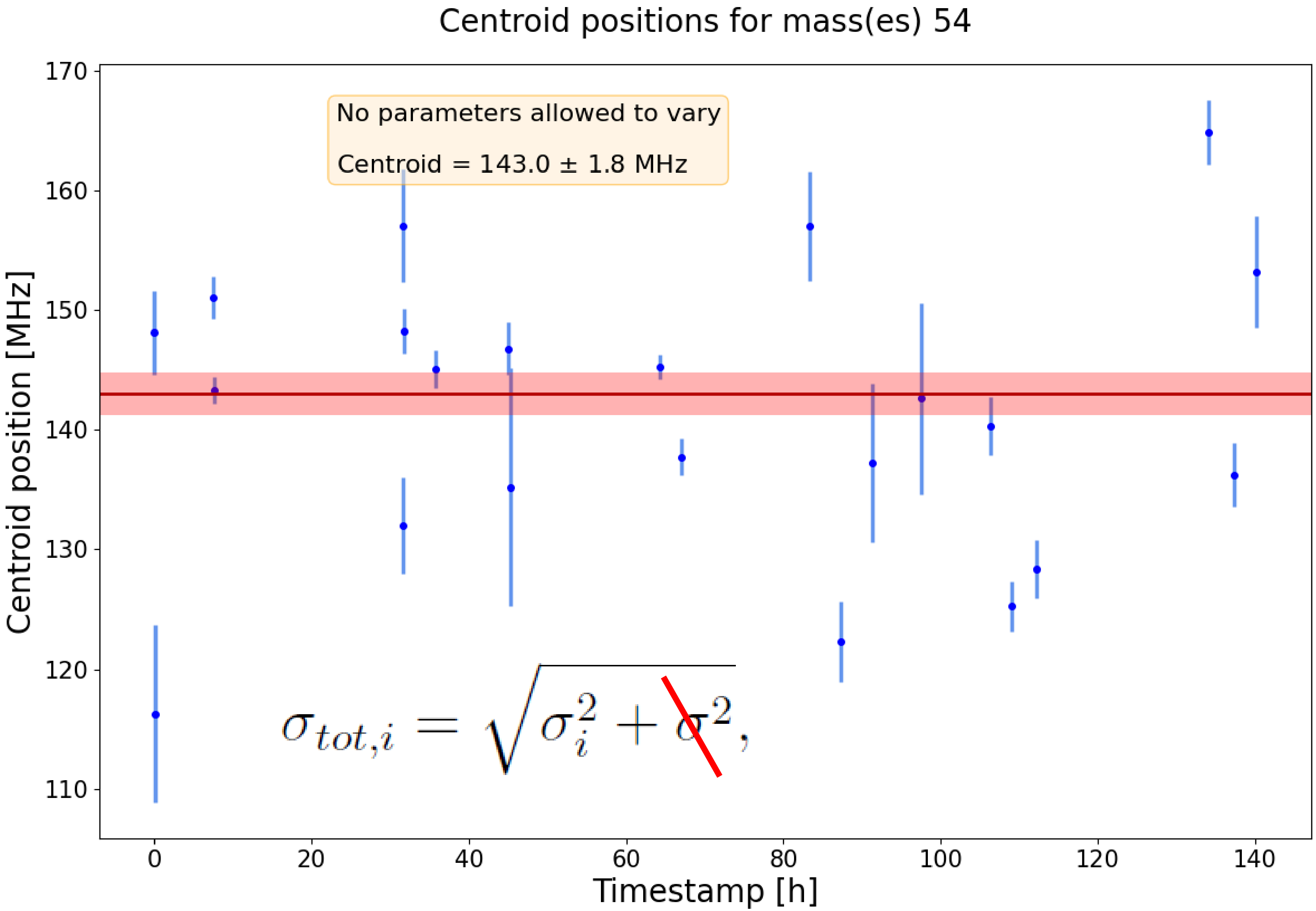

Departement Natuurkunde en Sterrenkunde, Instituut Kern- en Stralingsfysica

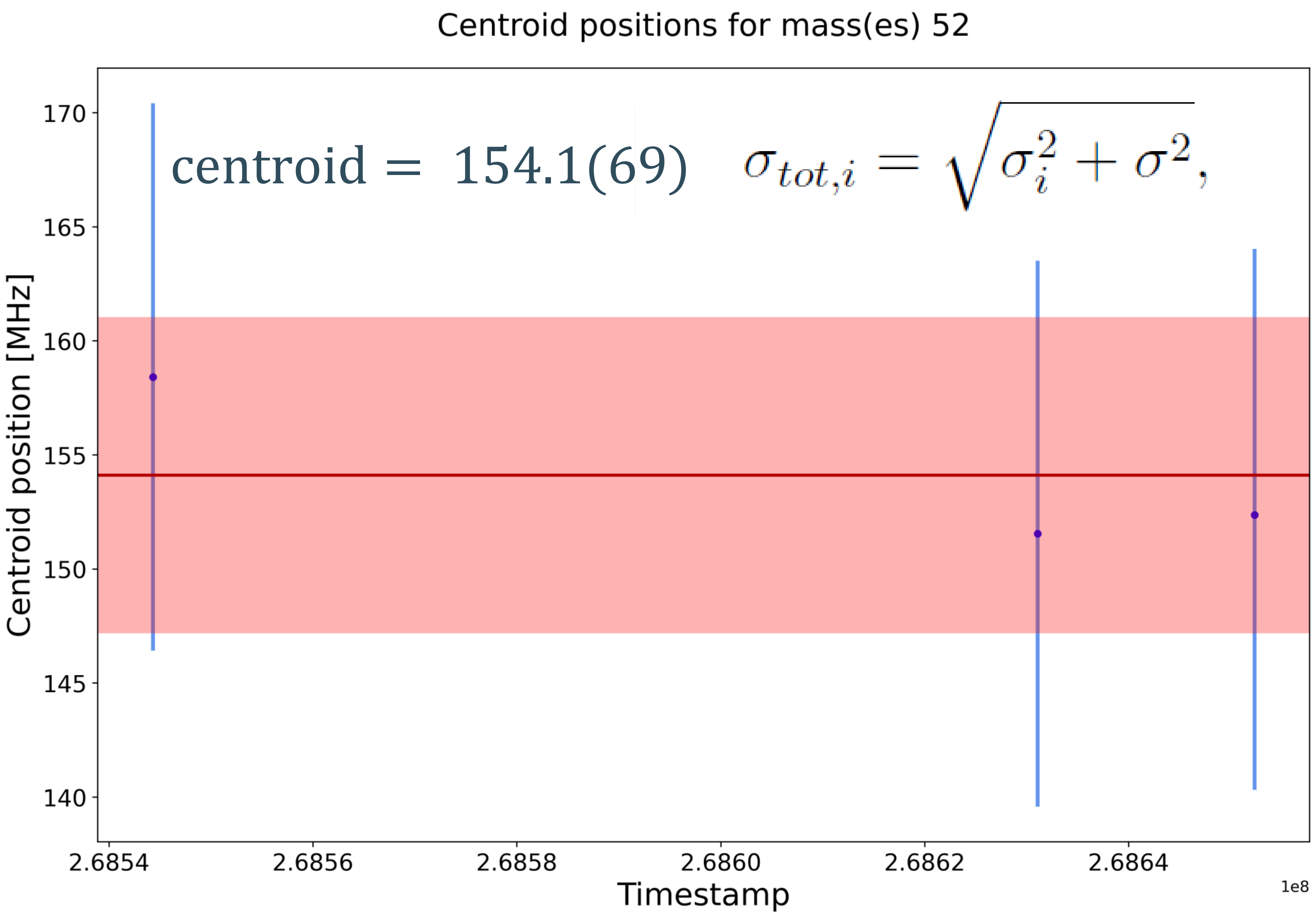

$$\text{centroid} = 154.1(69) \qquad \sigma_{tot,i} = \sqrt{\sigma_i^2 + \sigma^2},$$

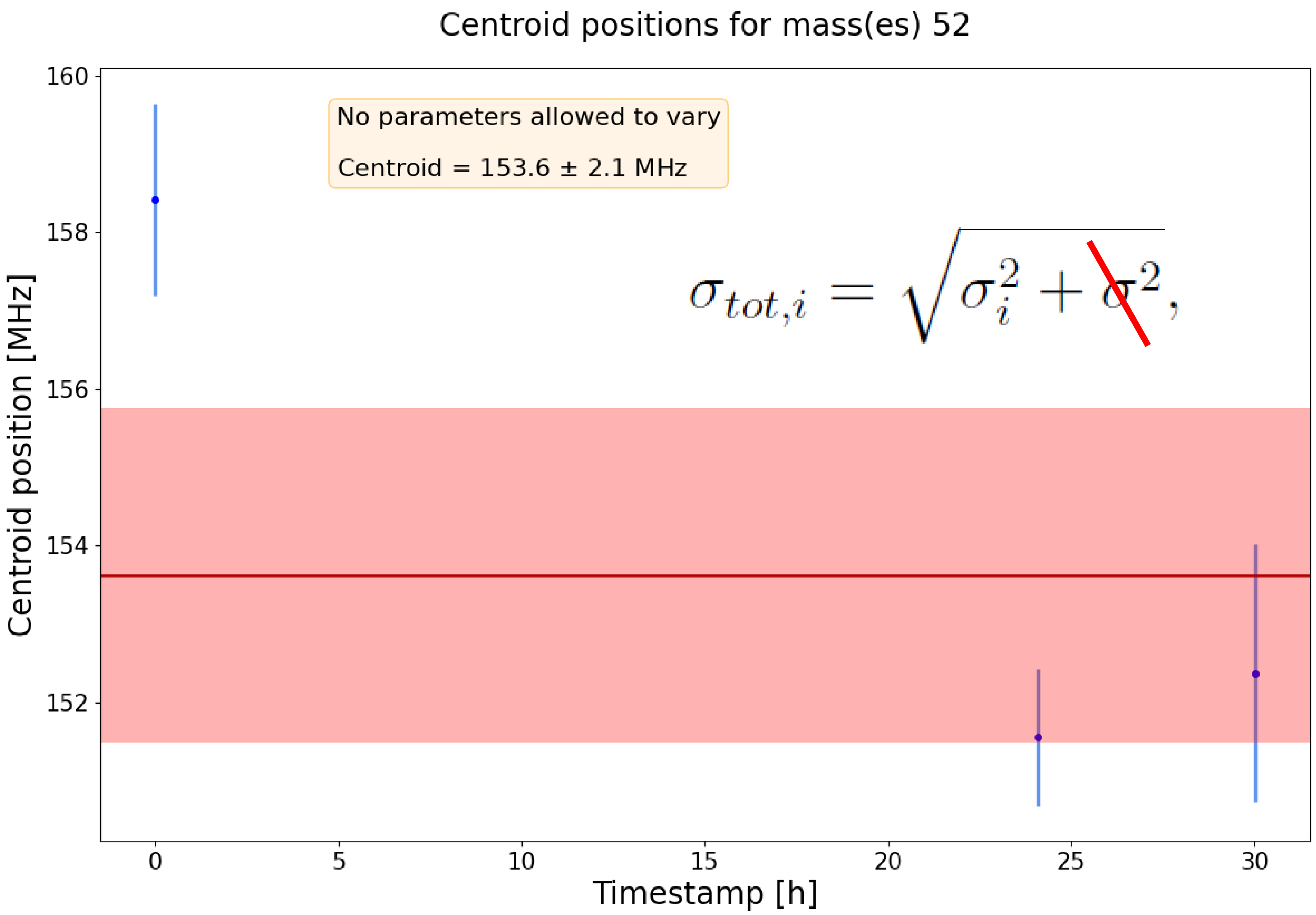

Centroid positions for mass(es) 52
No parameters allowed to vary
Centroid = 153.6 ± 2.1 MHz
$\sigma_{tot,i} = \sqrt{\sigma_i^2 + \sigma^2},$
Centroid position [MHz]
160
158
156
154
152
0
5
10
15
20
25
30
Timestamp [h]

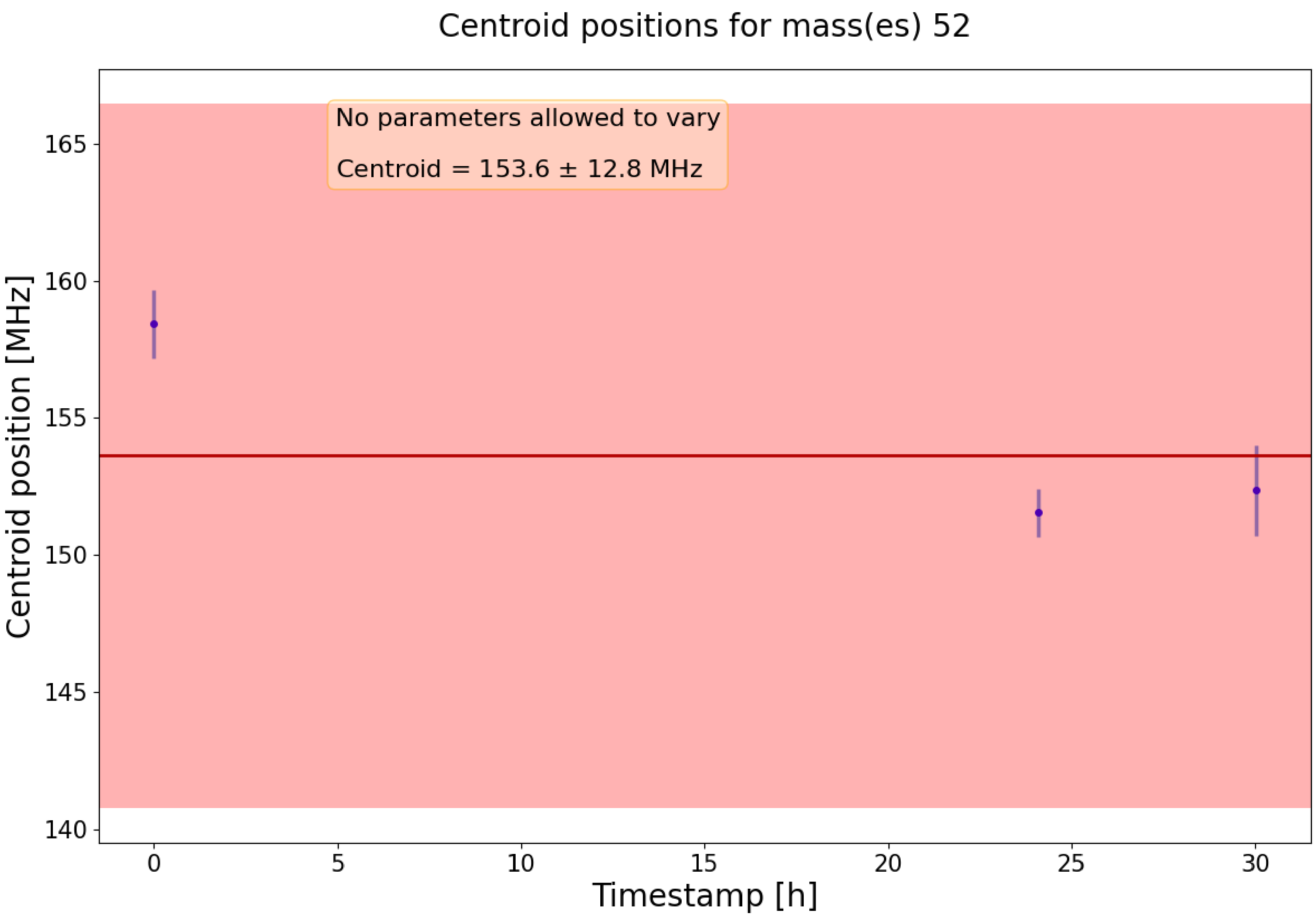
Centroid positions for mass(es) 52
No parameters allowed to vary
Centroid = 153.6 ± 12.8 MHz
Centroid position [MHz]
165
160
155
150
145
140
0
5
10
15
20
25
30
Timestamp [h]

Contents

Departement Natuurkunde en Sterrenkunde, Instituut Kern- en Stralingsfysica

KU LEUVEN